as the primary target, followed by the epimutation (hypomethylation) of the *MEG3*-DMR after fertilization; and (2) Loss of the hypermethylated DMRs of paternal origin has no effect on the imprinting status [2,26], so that upd(14)mat-like phenotype is primarily ascribed to the additive effects of loss of functional *DLK1* and *RTL1* from the paternally derived chromosome (the effects of loss of *DIO3* appears to be minor, if any [2,35]). Although the *MEGs* expression dosage is predicted to be normal in Deletion-4 and Deletion-5 and doubled in Epimutation-2 as well as in upd(14)mat, it remains to be determined whether the difference in the *MEGs* expression dosage has major clinical effects or not. (C) Normal and upd(14)pat/mat subjects.
Found at: doi:10.1371/journal.pgen.1000992.s003 (2.72 MB TIF)

Table S1 The results of microsatellite and SNP analyses.
Found at: doi:10.1371/journal.pgen.1000992.s004 (0.19 MB DOC)

Table S2 Clinical features in the mother of patient 1.
Found at: doi:10.1371/journal.pgen.1000992.s005 (0.09 MB DOC)

Table S3 Primers utilized in the present study.
Found at: doi:10.1371/journal.pgen.1000992.s006 (0.14 MB DOC)

Author Contributions

Conceived and designed the experiments: MK ACFS TO. Performed the experiments: MK MF KM FK. Analyzed the data: MK TO. Contributed reagents/materials/analysis tools: MJO AJG YW OA NM KM TO. Wrote the paper: TO.

References

1. da Rocha ST, Edwards CA, Ito M, Ogata T, Ferguson-Smith AC (2008) Genomic imprinting at the mammalian Dlk1-Dio3 domain. Trends Genet 24: 306–316.
2. Kagami M, Sekita Y, Nishimura G, Irie M, Kato F, et al. (2008) Deletions and epimutations affecting the human 14q32.2 imprinted region in individuals with paternal and maternal upd(14)-like phenotypes. Nat Genet 40: 237–242.
3. Kagami M, Yamazawa K, Matsubara K, Matsuo N, Ogata T (2008) Placentomegaly in paternal uniparental disomy for human chromosome 14. Placenta 29: 760–761.
4. Kotzot D (2004) Maternal uniparental disomy 14 dissection of the phenotype with respect to rare autosomal recessively inherited traits, trisomy mosaicism, and genomic imprinting. Ann Genet 47: 251–260.
5. Temple IK, Shrubb V, Lever M, Bullman H, Mackay DJ (2007) Isolated imprinting mutation of the DLK1/GTL2 locus associated with a clinical presentation of maternal uniparental disomy of chromosome 14. J Med Genet 44: 637–640.
6. Buiting K, Kanber D, Martín-Subero JI, Lieb W, Terhal P, et al. (2008) Clinical features of maternal uniparental disomy 14 in patients with an epimutation and a deletion of the imprinted DLK1/GTL2 gene cluster. Hum Mutat 29: 1141–1146.
7. Hosoki K, Ogata T, Kagami M, Tanaka T, Saitoh S (2008) Epimutation (hypomethylation) affecting the chromosome 14q32.2 imprinted region in a girl with upd(14)mat-like phenotype. Eur J Hum Genet 16: 1019–1023.
8. Zechner U, Kohlschmidt N, Rittner G, Damatova N, Beyer V, et al. (2009) Epimutation at human chromosome 14q32.2 in a boy with a upd(14)mat-like clinical phenotype. Clin Genet 75: 251–258.
9. Li E, Beard C, Jaenisch R (1993) Role for DNA methylation in genomic imprinting. Nature 366: 362–365.
10. Rosa AL, Wu YQ, Kwabi-Addo B, Coveler KJ, Reid Sutton V, et al. (2005) Allele-specific methylation of a functional CTCF binding site upstream of MEG3 in the human imprinted domain of 14q32. Chromosome Res 13: 809–818.
11. Wylie AA, Murphy SK, Orton TC, Jirtle RL (2000) Novel imprinted DLK1/GTL2 domain on human chromosome 14 contains motifs that mimic those implicated in IGF2/H19 regulation. Genome Res 10: 1711–1718.
12. Tierling S, Dalbert S, Schoppenhorst S, Tsai CE, Oliger S, et al. (2007) High-resolution map and imprinting analysis of the Gtl2-Dnchc1 domain on mouse chromosome 12. Genomics 87: 225–235.
13. Takada S, Paulsen M, Tevendale M, Tsai CE, Kelsey G, et al. (2002) Epigenetic analysis of the Dlk1-Gtl2 imprinted domain on mouse chromosome 12: implications for imprinting control from comparison with Igf2-H19. Hum Mol Genet 11: 77–86.
14. Ohlsson R, Renkawitz R, Lobanenkov V (2001) CTCF is a uniquely versatile transcription regulator linked to epigenetics and disease. Trends Genet 17: 520–527.
15. Hark AT, Schoenherr CJ, Katz DJ, Ingram RS, Levorse JM, et al. (2000) CTCF mediates methylation-sensitive enhancer-blocking activity at the H19/Igf2 locus. Nature 405: 486–489.
16. Kanduri C, Pant V, Loukinov D, Pugacheva E, Qi CF, et al. (2000) Functional association of CTCF with the insulator upstream of the H19 gene is parent of origin-specific and methylation-sensitive. Curr Biol 10: 853–856.
17. da Rocha ST, Tevendale M, Knowles E, Takada S, Watkins M, et al. (2007) Restricted co-expression of Dlk1 and the reciprocally imprinted non-coding RNA, Gtl2: implications for cis-acting control. Dev Biol 306: 810–823.
18. Wan LB, Pan H, Hannenhalli S, Cheng Y, Ma J, et al. (2008) Maternal depletion of CTCF reveals multiple functions during oocyte and preimplantation embryo development. Development 135: 2729–2738.
19. Ideraabdullah FY, Vigneau S, Bartolomei MS (2008) Genomic imprinting mechanisms in mammals. Mutat Res 647: 77–85.
20. Fitzpatrick GV, Pugacheva EM, Shin JY, Abdullaev Z, Yang Y, et al. (2007) Allele-specific binding of CTCF to the multipartite imprinting control region KvDMR1. Mol Cell Biol 27: 2636–2647.
21. Horsthemke B, Wagstaff J (2008) Mechanisms of imprinting of the Prader-Willi/Angelman region. Am J Med Genet A 146A: 2041–2052.
22. Lin SP, Coan P, da Rocha ST, Seitz H, Cavaille J, et al. (2007) Differential regulation of imprinting in the murine embryo and placenta by the Dlk1-Dio3 imprinting control region. Development 134: 417–426.
23. Coan PM, Burton GJ, Ferguson-Smith AC (2005) Imprinted genes in the placenta–a review. Placenta 26 Suppl A: S10–20.
24. Georgiades P, Watkins M, Surani MA, Ferguson-Smith AC (2000) Parental origin-specific developmental defects in mice with uniparental disomy for chromosome 12. Development 127: 4719–4728.
25. Takada S, Tevendale M, Baker J, Georgiades P, Campbell E, et al. (2000) Delta-like and gtl2 are reciprocally expressed, differentially methylated linked imprinted genes on mouse chromosome 12. Curr Biol 10: 1135–1138.
26. Lin SP, Youngson N, Takada S, Seitz H, Reik W, et al. (2003) Asymmetric regulation of imprinting on the maternal and paternal chromosomes at the Dlk1-Gtl2 imprinted cluster on mouse chromosome 12. Nat Genet 35: 97–102.
27. Takahashi N, Okamoto A, Kobayashi R, Shirai M, Obata Y, et al. (2009) Deletion of Gtl2, imprinted non-coding RNA, with its differentially methylated region induces lethal parent-origin-dependent defects in mice. Hum Mol Genet 18: 1879–1888.
28. Lewis A, Mitsuya K, Umlauf D, Smith P, Dean W, et al. (2004) Imprinting on distal chromosome 7 in the placenta involves repressive histone methylation independent of DNA methylation. Nat Genet 36: 1291–1295.
29. Umlauf D, Goto Y, Cao R, Cerqueira F, Wagschal A, et al. (2004) Imprinting along the Kcnq1 domain on mouse chromosome 7 involves repressive histone methylation and recruitment of Polycomb group complexes. Nat Genet 36: 1296–1300.
30. Sekita Y, Wagatsuma H, Irie M, Kobayashi S, Kohda T, et al. (2006) Aberrant regulation of imprinted gene expression in Gtl2lacZ mice. Cytogenet. Genome Res 113: 223–229.
31. Steshina EY, Carr MS, Glick EA, Yevtodiyenko A, Appelbe OK, et al. (2006) Loss of imprinting at the Dlk1-Gtl2 locus caused by insertional mutagenesis in the Gtl2 5′ region. BMC Genet 7: 44.
32. Charlier C, Segers K, Karim L, Shay T, Gyapay G, et al. (2001) The callipyge mutation enhances the expression of coregulated imprinted genes in cis without affecting their imprinting status. Nat Genet 27: 367–369.
33. Georges M, Charlier C, Cockett N (2003) The callipyge locus: evidence for the trans interaction of reciprocally imprinted genes. Trends Genet 19: 248–252.
34. Moon YS, Smas CM, Lee K, Villena JA, Kim KH, et al. (2002) Mice lacking paternally expressed Pref-1/Dlk1 display growth retardation and accelerated adiposity. Mol Cell Biol 22: 5585–5592.
35. Tsai CE, Lin SP, Ito M, Takagi N, Takada S, et al. (2002) Genomic imprinting contributes to thyroid hormone metabolism in the mouse embryo. Curr Biol 12: 1221–1226.
36. Sekita Y, Wagatsuma H, Nakamura K, Ono R, Kagami M, et al. (2008) Role of retrotransposon-derived imprinted gene, Rtl1, in the feto-maternal interface of mouse placenta. Nat Genet 40: 243–248.
37. Seitz H, Youngson N, Lin SP, Dalbert S, Paulsen M, et al. (2003) Imprinted microRNA genes transcribed antisense to a reciprocally imprinted retrotransposon-like gene. Nat Genet 34: 261–262.
38. Davis E, Caiment F, Tordoir X, Cavaillé J, Ferguson-Smith A, et al. (2005) RNAi-mediated allelic trans-interaction at the imprinted Rtl1/Peg11 locus. Curr Biol 15: 743–749.

JMG Online First, published on August 3, 2010 as 10.1136/jmg.2010.079343

Parthenogenetic chimaerism/mosaicism with a Silver-Russell syndrome-like phenotype

K Yamazawa,[1,2] K Nakabayashi,[3] M Kagami,[1] T Sato,[1] S Saitoh,[4] R Horikawa,[5] N Hizuka,[6] T Ogata[1]

► Additional figures, tables and an appendix are published online only. To view these files, please visit the journal online (http://jmg.bmj.com).

[1]Departments of Endocrinology and Metabolism, National Research Institute for Child Health and Development, Tokyo, Japan
[2]Department of Physiology, Development & Neuroscience, University of Cambridge, Cambridge, UK
[3]Maternal-Fetal Biology, National Research Institute for Child Health and Development, Tokyo, Japan
[4]Department of Pediatrics, Hokkaido University Graduate School of Medicine, Sapporo, Japan
[5]Division of Endocrinology and Metabolism, National Children's Hospital, Tokyo, Japan
[6]Department of Medicine, Institute of Clinical Endocrinology, Tokyo Women's Medical University, Tokyo, Japan

Correspondence to
Dr Tsutomu Ogata, Department of Endocrinology and Metabolism, National Research Institute for Child Health and Development, 2-10-1 Ohkura, Setagaya, Tokyo 157-8535, Japan; tomogata@nch.go.jp

Received 20 March 2010
Revised 6 May 2010
Accepted 8 May 2010

ABSTRACT

Introduction We report a 34-year-old Japanese female with a Silver-Russell syndrome (SRS)-like phenotype and a mosaic Turner syndrome karyotype (45,X/46,XX).

Methods/Results Molecular studies including methylation analysis of 17 differentially methylated regions (DMRs) on the autosomes and the *XIST*-DMR on the X chromosome and genome-wide microsatellite analysis for 96 autosomal loci and 30 X chromosomal loci revealed that the 46,XX cell lineage was accompanied by maternal uniparental isodisomy for all chromosomes (upid(AC)mat), whereas the 45,X cell lineage was associated with biparentally derived autosomes and a maternally derived X chromosome. The frequency of the 46,XX upid(AC)mat cells was calculated as 84% in leukocytes, 56% in salivary cells, and 18% in buccal epithelial cells.

Discussion The results imply that a parthenogenetic activation took place around the time of fertilisation of a sperm missing a sex chromosome, resulting in the generation of the upid(AC)mat 46,XX cell lineage by endoreplication of one blastomere containing a female pronucleus and the 45,X cell lineage by union of male and female pronuclei. It is likely that the extent of overall (epi)genetic aberrations exceeded the threshold level for the development of SRS phenotype, but not for the occurrence of other imprinting disorders or recessive Mendelian disorders.

Although a mammal with maternal uniparental disomy for all chromosomes (upd(AC)mat) is incompatible with life because of genomic imprinting,[1] a mammal with a upd(AC)mat cell lineage could be viable in the presence of a co-existing normal cell lineage. In the human, Strain *et al*[2] have reported 46,XX peripheral blood cells with maternal uniparental isodisomy for all chromosomes (upid(AC)mat) in a 1.2-year-old phenotypically male patient with aggressive behaviour, hemifacial hypoplasia and normal birth weight. Because of the 46,XX disorders of sex development, detailed molecular studies were performed, revealing the presence of a normal 46,XY cell lineage in a vast majority of skin fibroblasts and a upid(AC)mat 46,XX cell lineage in nearly all blood cells. In addition, although the data are insufficient to draw a definitive conclusion, Horike *et al*[3] have also identified 46,XX peripheral blood cells with possible upd(AC)mat in a phenotypically male patient through methylation analyses for plural differentially methylated regions (DMRs) in 11 patients with Silver–Russell syndrome (SRS)-like phenotype. This patient was found to have a normal 46,XY cell lineage and a triploid 69,XXY cell lineage in skin fibroblasts.

However, such patients with a upd(AC)mat cell lineage remain extremely rare, and there is no report describing a human with such a cell lineage in the absence of a normal cell lineage. Here, we report a female patient with a upid(AC)mat 46,XX cell lineage and a non-upd 45,X cell lineage who was identified through genetic screenings of 103 patients with SRS-like phenotype.

MATERIALS AND METHODS

Case report

This Japanese female patient was conceived naturally and born at 40 weeks of gestation by a normal vaginal delivery. At birth, her length was 44.0 cm (−3.1 SD), her weight 2.1 kg (−2.9 SD) and her occipitofrontal head circumference (OFC) 30.5 cm (−2.3 SD). The parents and the younger brother were clinically normal (the father died from a traffic accident).

At 2 years of age, she was referred to us because of growth failure. Her height was 77.7 cm (−2.5 SD), her weight 8.45 kg (−2.6 SD) and her OFC 43.5 cm (−2.5 SD). Physical examination revealed several SRS-like somatic features such as triangular face, right hemihypoplasia and bilateral fifth finger clinodactyly. She also had developmental retardation, with a developmental quotient of 56. Endocrine studies for short stature were normal as were radiological studies. Cytogenetic analysis using lymphocytes indicated a low-grade mosaic Turner syndrome (TS) karyotype, 45,X[3]/46,XX[47]. Thus, a screening of TS phenotype[4] was performed, detecting horseshoe kidney but no body surface features or cardiovascular lesion. Chromosome analysis was repeated at 6 and 32 years of age using lymphocytes, revealing a 45,X[8]/46,XX[92] karyotype and a 45,X[12]/46,XX[88] karyotype, respectively. On the last examination at 34 years of age, her height was 125.0 cm (−6.2 SD), her weight 37.5 kg (−2.0 SD) and her OFC 51.2 cm (−2.8 SD). She was engaged in a simple work and was able to get on her daily life for herself.

Sample preparation

This study was approved by the Institutional Review Board Committees at National Center for Child health and Development. After obtaining written informed consent, genomic DNA was extracted from leukocytes of the patient, the mother and the brother and from salivary cells, which comprise ~40% of buccal epithelial cells and ~60% of leukocytes,[5] of the patient. Lymphocyte metaphase spreads and leukocyte RNA were also

obtained from the patient. Leukocytes of healthy adults and patients with imprinting disorders were utilised for controls.

Primers and probes

The primers utilised in this study are summarised in supplementary methods and supplementary tables 1–3.

DMR analyses

We first performed bio-combined bisulfite restriction analysis (COBRA)[6] and bisulfite sequencing of the *H19*-DMR (A) on chromosome 11p15.5 by the previously described methods[7] and methylation-sensitive PCR analysis of the *MEST*-DMR (A) on chromosome 7q32.2 by the previously described methods[8] with minor modifications (the methylated and unmethylated allele-specific primers were designed to yield PCR products of different sizes, and the PCR products were visualised on the 2100 Bioanalyzer (Agilent, Santa Clara, California, USA)). This was because hypomethylation (epimutation) of the normally methylated *H19*-DMR of paternal origin and maternal uniparental disomy 7 are known to account for 35–65% and 5–10% of SRS patients, respectively.[9 10] In addition, fluorescence in situ hybridisation (FISH) analysis was performed with a ~84-kb RP5-998N23 probe containing the *H19*-DMR (BACPAC Resources Center, Oakland, California, USA). We also examined multiple other DMRs by bio-COBRA. The ratio of methylated clones (the methylation index) was calculated using peak heights of digested and undigested fragments on the 2100 Bioanalyzer using 2100 expert software.

Genome-wide microsatellite analysis

Microsatellite analysis was performed for 96 autosomal loci and 30 X chromosomal loci. The segment encompassing each locus was PCR-amplified, and the PCR product size was determined on the ABI PRISM 310 autosequencer using GeneScan software (Applied Biosystems, Foster City, California, USA).

PCR analysis for Y chromosomal loci

Standard PCR was performed for six Y chromosomal loci. The PCR products were electrophoresed using the 2100 Bioanalyzer.

Expression analysis

Quantitative real-time reverse transcriptase PCR analysis was performed for three paternally expressed genes (*IGF2*, *SNRPN* and *ZAC1*) and four maternally expressed genes (*H19*, *MEG3*, *PHLDA2* and *CDKN1C*) that are known to be variably (usually weakly) expressed in leukocytes (UniGene, http://www.ncbi.nlm.nih.gov/sites/entrez?db=unigene), using an ABI Prism 7000 Sequence Detection System (Applied Biosystems). *TBP* and *GAPDH* were utilised as internal controls.

RESULTS

DMR analyses

In leukocytes, the bio-COBRA indicated severely hypomethylated *H19*-DMR, and bisulfite sequencing combined with *rs2251375* SNP typing for 30 clones revealed maternal origin of 29 hypomethylated clones and non-maternal (paternal) origin of a single methylated clone in this patient (figure 1A). Thus, the marked hypomethylation of the *H19*-DMR was caused by predominance of maternally derived clones rather than hypomethylation of the *H19*-DMR of paternal origin. FISH analysis for 100 lymphocyte metaphase spreads excluded an apparent deletion of the paternally derived *H19*-DMR or duplication of the maternally derived *H19*-DMR (Supplementary figure 1). Methylation-sensitive PCR amplification for the *MEST*-DMR delineated a major peak for the methylated allele and a minor peak for the unmethylated allele (figure 1B). This also indicated the predominance of maternally derived clones and the co-existence of a minor portion of paternally derived clones. Furthermore, autosomal DMRs invariably exhibited markedly abnormal methylation patterns consistent with predominance of maternally inherited DMRs, whereas the methylation index of the *XIST*-DMR on the X chromosome remained within the female reference range (figure 1C). The abnormal methylation patterns were less obvious in salivary cells (thus, in buccal epithelial cells) than in leukocytes, except for the methylation index for the *XIST*-DMR that mildly exceeded the female reference range (figure 1A–C).

Microsatellite analysis

Major peaks consistent with maternal uniparental isodisomy and minor peaks of non-maternal (paternal) origin were identified for at least one locus on each autosome, with the minor peaks of non-maternal origin being more obvious in salivary cells than in leukocytes (figure 1D and supplementary table 4). Furthermore, the frequency of the upid(AC)mat cells was calculated as 84% in leukocytes, 56% in salivary cells and 18% in epithelial buccal cells, using the area under curves for the maternally and the non-maternally inherited peaks (supplementary note). Such minor peaks of non-maternal origin were not detected for all the 30 X chromosomal loci examined.

PCR analysis for Y chromosomal loci

PCR amplification failed to detect any trace of Y chromosome-specific bands in leukocytes and salivary cells (Supplementary figure 2).

Expression analysis

Expression analysis using control leukocytes indicated that, of the seven examined genes, *SNRPN* expression alone was strong enough to allow for a precise assessment (Supplementary figure 3). *SNRPN* expression was extremely low in this patient (figure 1E).

DISCUSSION

These results imply that this patient had a upid(AC)mat 46,XX cell lineage and a non-upd 45,X cell lineage. Indeed, methylation patterns of the *XIST*-DMR is explained by assuming that the two X chromosomes in the upid(AC)mat cells undergo random X-inactivation and that 45,X cells with the methylated *XIST*-DMR on a single active X chromosome[11] are relatively prevalent in buccal epithelial cells. Furthermore, lack of non-maternally derived minor peaks for microsatellite loci on the X chromosome is explained by assuming that the two X chromosomes in the upid(AC)mat cells and the single X chromosome in the 45,X cells are derived from a common X chromosome of maternal origin, with no paternally derived sex chromosome. It is likely, therefore, that a parthenogenetic activation took place around the time of fertilisation of a sperm missing a sex chromosome, resulting in the generation of the 46,XX cell lineage with upid (AC)mat by endoreplication (the replication of DNA without the subsequent completion of mitosis) of one blastomere containing a female pronucleus and the 45,X cell lineage with biparentally derived autosomes and a maternally derived X chromosome by union of male and female pronuclei (figure 2), although it is also possible that a paternally derived sex chromosome was present in the sperm but was lost from the normal

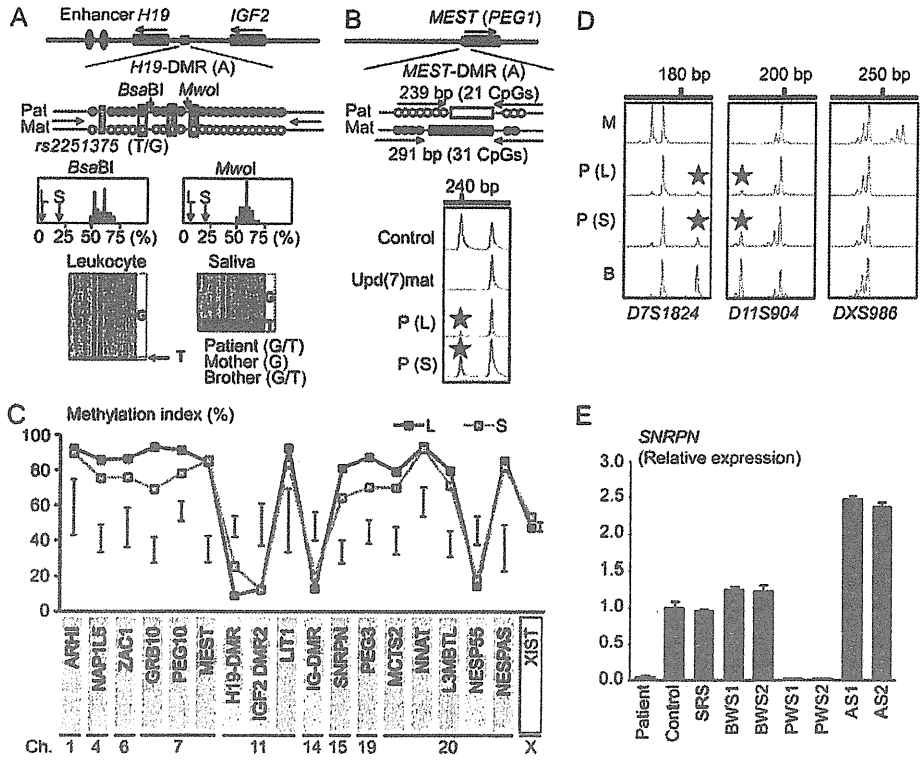

Figure 1 Representative molecular results. Pat, paternally derived allele; Mat, maternally derived allele; P, patient; M, mother; B, brother; L, leukocytes; and S, salivary cells. Filled and open circles in A and B represent methylated and unmethylated cytosine residues at the CpG dinucleotides, respectively. A. Methylation patterns of the *H19*-DMR (A) harbouring 23 CpG dinucleotides and the T/G SNP (*rs2251375*) (a grey box). The PCR products are digested with *Bsa*BI when the cytosine at the sixth CpG dinucleotide (highlighted in yellow) is methylated and with *Mwo*I when the two cytosines at the ninth and the 11th CpG dinucleotides (highlighted in orange) are methylated. For the bio-COBRA data, the black histograms represent the distribution of methylation indices (%) in 50 control participants, and L and S denote the methylation indices for leukocytes and salivary cells of this patient, respectively. For the bisulfite sequencing data, each line indicates a single clone. B. Methylated and unmethylated allele-specific PCR analysis for the *MEST*-DMR (A). In a control participant, the PCR products for methylated and unmethylated alleles are delineated, and the unequal amplification is consistent with a short product being more easily amplified than a long product. In a previously reported patient with upd(7)mat,[8] the methylated allele only is amplified. In this patient, major peaks for the methylated allele and minor peaks for the unmethylated allele (red asterisks) are detected. C. Methylation patterns for the 18 DMRs examined. The DMRs highlighted in blue and pink are methylated after paternal and maternal transmissions, respectively. The black vertical bars indicate the reference data (maximum—minimum) in 20 normal control participants, using leukocyte genomic DNA (for the *XIST*-DMR, 16 female data are shown). D. Representative microsatellite analysis. Minor peaks (red asterisks) have been identified for *D7S1824* and *D11S904* but not for *DXS986* of the patient. Since the peaks for *D7S1824* and *D11S904* are absent in the mother and clearly present in the brother, they are assessed to be of paternal origin. E. Relative expression level (mean ± SD) of *SNRPN* on chromosome 15. The data have been normalised against *TBP*. SRS, an SRS patient with an epimutation (hypomethylation) of the *H19*-DMR; BWS1, a BWS patient with an epimutation (hypermethylation) of the *H19*-DMR; BWS2, a BWS patient with upd(11)pat; PWS1, a PWS patient with upd(15)mat; PWS2, a PWS patient with an epimutation (hypermethylation) of the *SNRPN*-DMR; AS1, an Angelman syndrome (AS) patient with upd(15)pat; and AS2, an AS patient with an epimutation (hypomethylation) of the *SNRPN*-DMR.

cell lineage at the very early developmental stage. Hence, in a strict sense, this patient is neither a chimera resulting from the fusion of two different zygotes nor a mosaic caused by a mitotic error of a single zygote. In this regard, a triploid cell stage is assumed in the generation of a upid(AC)mat cell lineage, and such triploid cells may have been detected in skin fibroblasts of the patient reported by Horike *et al*.[3]

The upid(AC)mat cells accounted for the majority of leukocytes even in adulthood of this patient, despite global negative selective pressure.[12 13] This phenomenon, though intriguing, would not be unexpected in human studies because leukocytes are usually utilised for genetic analyses. Rather, if the upid(AC)mat cells were barely present in leukocytes, they would not have been detected. It is likely, therefore, that upid(AC)mat cells have occupied a relatively large portion of the definitive haematopoietic tissues primarily as a stochastic event. Furthermore, parthenogenetic chimera mouse studies have revealed that parthenogenetic cells are found at a relatively high frequency in some tissues/organs including blood and are barely identified in other tissues/organs such as skeletal muscle and liver.[13] Such a possible tissue-specific selection in favour of the preservation of parthenogenetic cells in the definitive haematopoietic tissues may also be relevant to the predominance of the upid(AC)mat cells in leukocytes. In addition, a reduced growth potential of 45,X cells[14] may also have contributed to the skewed ratio of the two cell lineages.

Clinical features of this patient would be determined by several factors. They include: (1) the ratio of two cell lineages in various tissues/organs, (2) the number of imprinted regions or DMRs relevant to the development of specific imprinting disorders (eg, plural regions/DMRs on chromosomes 7 and 11 for SRS[9 10] and a single region/DMR on chromosome 15 for Prader—Willi syndrome (PWS)),[15] (3) the degree of clinical effects of dysregulated imprinted regions/DMRs (an (epi)dominant effect has been

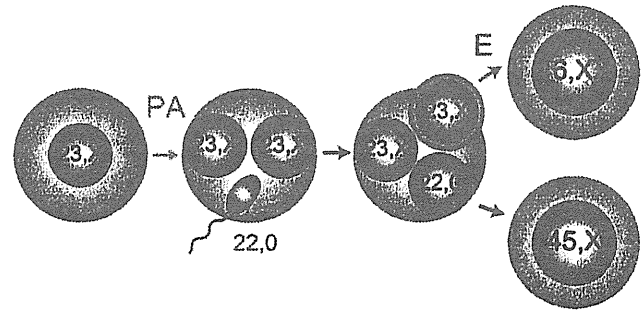

Figure 2 Schematic representation of the generation of the upid(AC)mat 46,XX cell lineage and the non-upd 45,X cell lineage. Polar bodies are not shown. PA, parthenogenetic activation; and E, endoreplication of one blastomere containing a female pronucleus.

assumed for the 11p15.5 imprinted regions including the *IGF2–H19* domain on the basis of SRS or Beckwith–Wiedemann syndrome (BWS) phenotype in patients with multilocus hypomethylation[16] and BWS-like phenotype in patients with a upid (AC)pat cell lineage,[17] a mirror image of a upid(AC)mat cell lineage), (4) expression levels of imprinted genes in upid(AC)mat cells (although *SNRPN* expression of this patient was consistent with upid(AC)mat cells being predominant in leukocytes, complicated expression patterns have been identified for several imprinted genes in androgenetic and parthenogenetic fetal mice, probably because of perturbed *cis*- and *trans*-acting regulatory mechanisms)[18] and (5) unmasking of possible maternally inherited recessive mutation(s) in upid(AC)mat cells.[19] Collectively, it appears that the extent of overall (epi)genetic aberrations exceeded the threshold level for the development of SRS phenotype and horseshoe kidney characteristic of TS[4] but remained below the threshold level for the occurrence of other imprinting disorders or recessive Mendelian disorders.

In summary, we identified a upid(AC)mat 46,XX cell lineage in a woman with an SRS-like phenotype and a 45,X cell lineage accompanied by autosomal haploid sets of biparental origin. This report will facilitate further identification of patients with a upid(AC)mat cell lineage and better clarification of the clinical phenotypes in such patients.

Acknowledgements We thank the patient and her family members for their participation in this study. We also thank Dr. Toshiro Nagai for providing us with blood samples of patients with Prader–Willi syndrome.

Funding This work was supported by grants from the Ministry of Health, Labor, and Welfare and from the Ministry of Education, Science, Sports and Culture.

Competing interests None.

Patient consent Obtained.

Ethics approval This study was conducted with the approval of the Institutional Review Board Committees at National Center for Child health and Development.

Contributors Drs Kazuki Yamazawa (first author) and Kazuhiko Nakabayashi (second author) contributed equally to this work.

Provenance and peer review Not commissioned; externally peer reviewed.

REFERENCES

1. **McGrath J,** Solter D. Completion of mouse embryogenesis requires both the maternal and paternal genomes. *Cell* 1984;**37**:179–83.
2. **Strain L,** Warner JP, Johnston T, Bonthron DT. A human parthenogenetic chimaera. *Nat Genet* 1995;**11**:164–9.
3. **Horike S,** Ferreira JC, Meguro-Horike M, Choufani S, Smith AC, Shuman C, Meschino W, Chitayat D, Zackai E, Scherer SW, Weksberg R. Screening of DNA methylation at the H19 promoter or the distal region of its ICR1 ensures efficient detection of chromosome 11p15 epimutations in Russell–Silver syndrome. *Am J Med Genet Part A* 2009;**149A**:2415–23.
4. **Styne D,** Grumbach M. Puberty: ontogeny, neuroendocrinology, physiology, and disorders. In: Kronenberg H, Melmed M, Polonsky K, Larsen P, eds. *Williams textbook of endocrinology*, 11th edn. Philadelphia: Saunders 2008:969–1166.
5. **Thiede C,** Prange-Krex G, Freiberg-Richter J, Bornhauser M, Ehninger G. Buccal swabs but not mouthwash samples can be used to obtain pretransplant DNA fingerprints from recipients of allogeneic bone marrow transplants. *Bone Marrow Transplant* 2000;**25**:575–7.
6. **Brena RM,** Auer H, Kornacker K, Hackanson B, Raval A, Byrd JC, Plass C. Accurate quantification of DNA methylation using combined bisulfite restriction analysis coupled with the Agilent 2100 Bioanalyzer platform. *Nucleic Acids Res* 2006;**34**:e17.
7. **Yamazawa K,** Kagami M, Nagai T, Kondoh T, Onigata K, Maeyama K, Hasegawa T, Hasegawa Y, Yamazaki T, Mizuno S, Miyoshi Y, Miyagawa S, Horikawa R, Matsuoka K, Ogata T. Molecular and clinical findings and their correlations in Silver–Russell syndrome: implications for a positive role of IGF2 in growth determination and differential imprinting regulation of the IGF2-H19 domain in bodies and placentas. *J Mol Med* 2008;**86**:1171–81.
8. **Yamazawa K,** Kagami M, Ogawa M, Horikawa R, Ogata T. Placental hypoplasia in maternal uniparental disomy for chromosome 7. *Am J Med Genet Part A* 2008;**146A**:514–16.
9. **Abu-Amero S,** Monk D, Frost J, Preece M, Stanier P, Moore GE. The genetic aetiology of Silver–Russell syndrome. *J Med Genet* 2008;**45**:193–9.
10. **Eggermann T,** Eggermann K, Schonherr N. Growth retardation versus overgrowth: Silver–Russell syndrome is genetically opposite to Beckwith–Wiedemann syndrome. *Trends Genet* 2008;**24**:195–204.
11. **Goto T,** Monk M. Regulation of X-chromosome inactivation in development in mice and humans. *Microbiol Mol Biol Rev* 1998;**62**:362–78.
12. **Nagy A,** Sass M, Markkula M. Systematic non-uniform distribution of parthenogenetic cells in adult mouse chimaeras. *Development* 1989;**106**:321–4.
13. **Fundele R,** Norris ML, Barton SC, Reik W, Surani MA. Systematic elimination of parthenogenetic cells in mouse chimeras. *Development* 1989;**106**:29–35.
14. **Verp MS,** Rosinsky B, Le Beau MM, Martin AO, Kaplan R, Wallemark CB, Otano L, Simpson JL. Growth disadvantage of 45, X and 46, X, del(X)(p11) fibroblasts. *Clin Genet* 1988;**33**:277–85.
15. **Horsthemke B,** Wagstaff J. Mechanisms of imprinting of the Prader–Willi/Angelman region. *Am J Med Genet A* 2008;**146A**:2041–52.
16. **Azzi S,** Rossignol S, Steunou V, Sas T, Thibaud N, Danton F, Le Jule M, Heinrichs C, Cabrol S, Gicquel C, Le Bouc Y, Netchine I. Multilocus methylation analysis in a large cohort of 11p15-related foetal growth disorders (Russell Silver and Beckwith Wiedemann syndromes) reveals simultaneous loss of methylation at paternal and maternal imprinted loci. *Hum Mol Genet* 2009;**18**:4724–33.
17. **Wilson M,** Peters G, Bennetts B, McGillivray G, Wu ZH, Poon C, Algar E. The clinical phenotype of mosaicism for genome-wide paternal uniparental disomy: two new reports. *Am J Med Genet Part A* 2008;**146A**:137–48.
18. **Ogawa H,** Wu Q, Komiyama J, Obata Y, Kono T. Disruption of parental-specific expression of imprinted genes in uniparental fetuses. *FEBS Lett* 2006;**580**:5377–84.
19. **Engel E.** A fascination with chromosome rescue in uniparental disomy: Mendelian recessive outlaws and imprinting copyrights infringements. *Eur J Hum Genet* 2006;**14**:1158–69.

RESEARCH LETTER

AMERICAN JOURNAL OF medical genetics PART A

Prenatal Findings of Paternal Uniparental Disomy 14: Delineation of Further Patient

Nobuhiro Suzumori,[1,2]* Tsutomu Ogata,[3] Eita Mizutani,[1,2] Yukio Hattori,[1] Keiko Matsubara,[3] Masayo Kagami,[3] and Mayumi Sugiura-Ogasawara[1]

[1]Department of Obstetrics & Gynecology, Nagoya City University Graduate School of Medicine, Nagoya, Japan

[2]Division of Molecular and Clinical Genetics, Nagoya City University Graduate School of Medicine, Nagoya, Japan

[3]Department of Endocrinology and Metabolism, National Research Institute for Child Health and Development, Tokyo, Japan

Received 5 March 2010; Accepted 2 August 2010

TO THE EDITOR:

Human chromosome 14q32.2 carries a cluster of imprinted genes including paternally expressed genes such as *DLK1* and *RTL1* and maternally expressed genes such as *MEG3* (alias *GTL2*) and *RTL1as* (*RTL1* antisense), together with the germline-derived intergenic differentially methylated region (IG-DMR) and the postfertilization-derived *MEG3*-DMR [da Rocha et al., 2008; Kagami et al., 2008a]. Consistent with this, paternal uniparental disomy 14 (upd(14)pat) results in a unique phenotype characterized by facial abnormality, small bell-shaped thorax with coat-hanger appearance of the ribs, abdominal wall defects, placentomegaly, and polyhydramnios [Kagami et al., 2008a,b], and maternal uniparental disomy 14 (upd(14)mat) leads to less-characteristic but clinically discernible features including growth failure [Kotzot, 2004; Kagami et al., 2008a].

For upd(14)pat, this condition has primarily been identified by the pathognomonic chest roentgenographic findings that are obtained immediately after birth because of severe respiratory dysfunction [Kagami et al., 2008a]. However, upd(14)pat has also been suspected prenatally by fetal radiological findings suggestive of small thorax and other characteristic findings [Curtis et al., 2006; Yamanaka et al., 2010]. Here, we report on prenatal findings in a hitherto unreported upd(14)pat patient. The results will serve to the prenatal identification of similarly affected patients and appropriate neonatal care including respiratory management.

A 41-year-old gravida 1, para 0 Japanese woman was referred to Nagoya City University Hospital because of polyhydramnios at 24 weeks of gestation. The polyhydramnios was severe and required repeated amnioreduction (1,600 ml at 26 weeks, 1,800 ml at 29 weeks, 2,000 ml at 32 weeks, and 2,100 ml at 35 weeks). The fetal urine volume was normal (5–12 ml per hr). At 28 weeks of gestation, 3D ultrasound studies were performed, delineating dysmorphic face, anteverted nares, micrognathia and small thorax characteristic of upd(14)pat (Fig. 1), although the differential diagnosis included Beckwith–Wiedemann syndrome and several types of skeletal dysplasia. Thereafter, ultrasound studies were weekly carried out, indicating almost normal fetal growth and normal umbilical artery Doppler.

How to Cite this Article:
Suzumori N, Ogata T, Mizutani E, Hattori Y, Matsubara K, Kagami M, Sugiura-Ogasawara M. 2010. Prenatal Findings of Paternal Uniparental Disomy 14: Delineation of Further Patient.
Am J Med Genet Part A 152A:3189–3192.

At 37 weeks of gestation, a 2,778 g male infant was delivered by cesarean because of fetal distress. The placenta was 1,384 g (gestational age-matched reference, 510 ± 98 g) [Kagami et al., 2008b]. The patient had severe asphyxia, and immediately received appropriate management including mechanical ventilation for 6 days and nasal directional positive airway pressure at the neonatal intensive care unit. At birth, physical examination revealed hairy forehead, blepharophimosis, depressed nasal bridge, anteverted nares, small ears, protruding philtrum, puckered lips, micrognathia, short webbed neck, joint contractures, and diastasis recti, and roentgenograms showed typical bell-shaped thorax with coat-hanger appearance of the ribs (Fig. 2). Coax valga or kyphoscoliosis was uncertain. Discharge from hospital was 35 days after birth. On the last examination at 8 months of age, the patient

*Correspondence to:
Nobuhiro Suzumori, M.D., Ph.D., Division of Molecular and Clinical Genetics, Department of Obstetrics 8601, Japan.
E-mail: og.n.suz@med.nagoya-cu.ac.jp
Published online 24 November 2010 in Wiley Online Library (wileyonlinelibrary.com)
DOI 10.1002/ajmg.a.33719

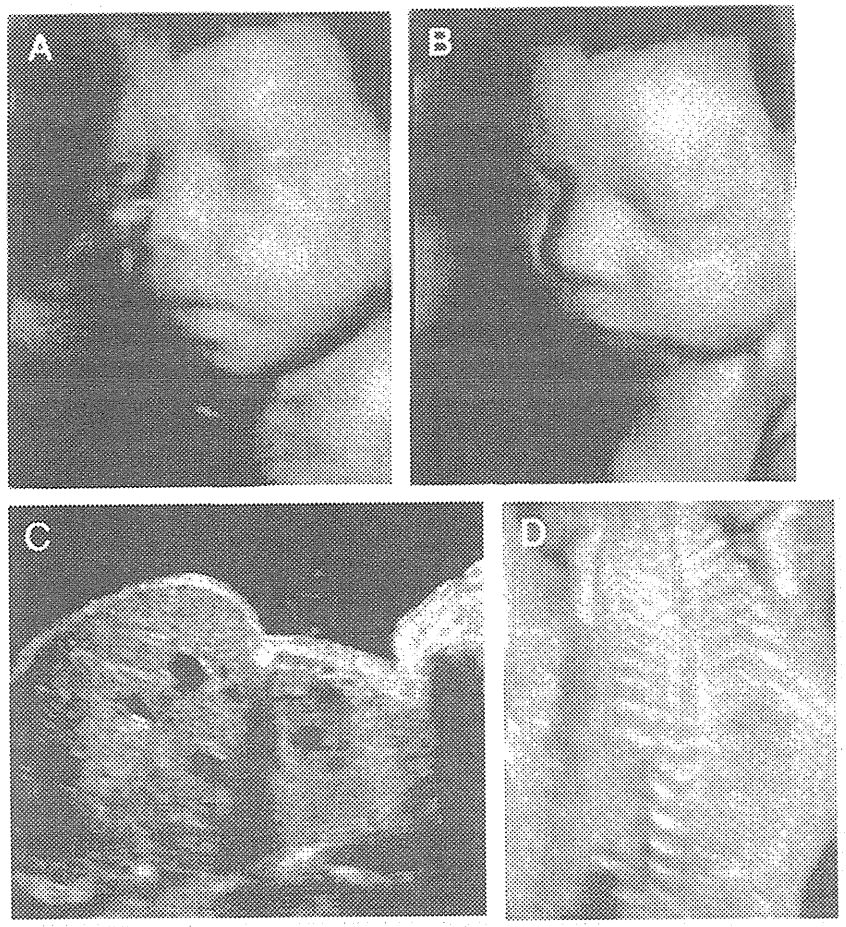

FIG. 1. Prenatal 3D findings at 28 weeks of gestation. A,B: Face appearance with blepharophimosis, depressed nasal bridge, anteverted nares, and micrognathia. C: Small thorax and polyhydramnios. D: Coat-hanger like appearance of the ribs.

required regular oropharyngeal suction and nasogastric tube feeding due to a poor swallowing reflex, and showed developmental delay. At the time of the last evaluation there was no seizure disorder.

To confirm the findings, cytogenetic and molecular studies were performed for the cord blood of the patient by the previously described methods [Kagami et al., 2008a]. This study was approved by the Institutional Review Board Committees at National Center for Child Health and Development and Nagoya City University, and performed after obtaining written informed consent. The karyotype was normal, and metaphase fluorescence in situ hybridization (FISH) analysis with a 202 kb BAC probe containing *DLK1* (RP11-566J3) and a 165 kb BAC probe containing *MG3* and *RTL1/RTL1as* (RP11-123M6) (http://bacpac.-chori.org/) delineated two signals with a similar intensity, respectively. Methylation analysis for bisulfite-treated genomic DNA indicated the presence of paternally derived hypermethylated IG-DMR (CG4 and CG6) and *MEG3*-DMR (CG7) and the absence of maternally derived hypomethylated DMRs. Furthermore, microsatellite analysis was performed using leukocyte genomic DNA of patient and parents, revealing uniparental paternal isodisomy for chromosome 14 (Table I, Fig. 3).

In this patient with molecularly confirmed upd(14)pat, ultrasound studies unequivocally showed typical upd(14)pat phenotypes such as thoracic abnormality and facial dysmorphic features. While this is the first report documenting the facial appearance of the affected fetus, small thorax has been suspected prenatally in five patients with upd(14)pat or epimutations of the IG-DMR and the *MEG3*-DMR, with coat-hanger appearance of the ribs being delineated in one patient [Curtis et al., 2006; Yamanaka et al., 2010]. In this regard, it is notable that polyhydramnios has invariably been identified in upd(14)pat by the second trimester [Kagami et al., 2008a]. It is recommended, therefore, to perform radiological studies for pregnant women with polyhydramnios, to suspect upd(14)pat-compatible clinical features of the fetus. This will permit appropriate counseling and delivery planning at a tertiary

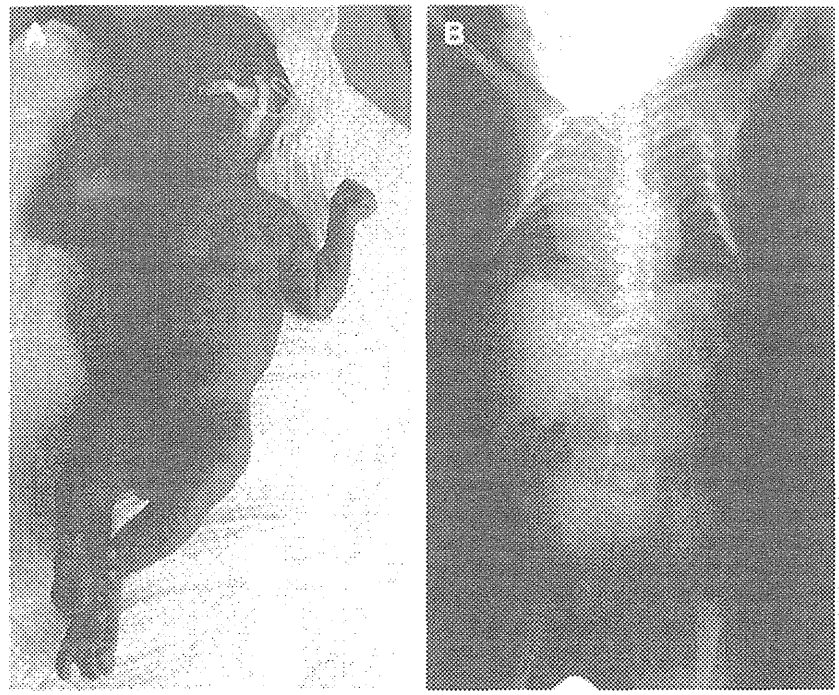

FIG. 2. Postnatal findings at 1 month of age. A: Front view. B: Chest roentgenogram showing bell-shaped thorax with coat-hanger appearance of the ribs.

center with neonatal intensive care as well as pertinent molecular studies using cord blood.

ACKNOWLEDGMENTS

We thank Dr. Saori Kaneko for her assistance in coordinating this research. We also acknowledge the cooperation of the patient's family in allowing us to publish their information.

TABLE 1. The Results of Microsatellite Analysis

Locus	Location	Mother	Patient	Father	Assessment
D14S80	14q12	98	98	98	N.I.
D14S608	14q12	200	194	194/210	Isodisomy
D14S588	14q23–24.1	114/126	114	114/122	N.I.
D14S617	14q32.12	139/169	143	143/165	Isodisomy
D14S250	14q32.2	159	159	159/167	N.I.
D14S1006	14q32.2	127/139	127	127/139	N.I.
D14S985	14q32.2	135/137	131	131/133	Isodisomy
D14S1010	14q32.33	134/142	142	142/144	N.I.
D14S1007	14q32.33	119	119	119	N.I.

N.I., not informative.
The Arabic numbers indicate the PCR product sizes in bp.
The imprinted region resides at 14q32.2.
D14S985 is located in the intron of *MEG3*.

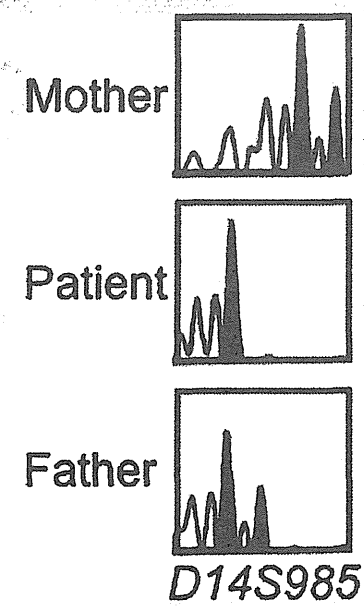

FIG. 3. Microsatellite analysis for *D14S985* residing in the intron of *MEG3*. One of the two peaks in the father is transmitted to the patient, and both of the two peaks in the mother are not inherited by the patient. The PCR fragment size: 135 and 137 bp in the mother, 131 bp in the patient, and 131 and 133 bp in the father. [Color figure can be viewed in the online issue, which is available at wileyonlinelibrary.com]

REFERENCES

Curtis L, Antonelli E, Vial Y, Rimensberger P, Merrer ML, Hinard C, Bottani A, Fokstuen S. 2006. Prenatal diagnostic indicators of paternal uniparental disomy 14. Prenat Diagn 26:662–666.

da Rocha ST, Edwards CA, Ito M, Ogata T, Ferguson-Smith AC. 2008. Genomic imprinting at the mammalian Dlk1-Dio3 domain. Trends Genet 24:306–316.

Kagami M, Sekita Y, Nishimura G, Irie M, Kato F, Okada M, Yamamori S, Kishimoto H, Nakayama M, Tanaka Y, Matsuoka K, Takahashi T, Noguchi M, Tanaka Y, Masumoto K, Utsunomiya T, Kouzan H, Komatsu Y, Ohashi H, Kurosawa K, Kosaki K, Ferguson-Smith AC, Ishino F, Ogata T. 2008a. Deletions and epimutations affecting the human 14q32.2 imprinted region in individuals with paternal and maternal upd(14)-like phenotypes. Nat Genet 40:237–242.

Kagami M, Yamazawa K, Matsubara K, Matsuo N, Ogata T. 2008b. Placentomegaly in paternal uniparental disomy for human chromosome 14. Placenta 29:760–761.

Kotzot D. 2004. Maternal uniparental disomy 14 dissection of the phenotype with respect to rare autosomal recessively inherited traits, trisomy mosaicism, and genomic imprinting. Ann Genet 47: 251–260.

Yamanaka M, Ishikawa H, Saito K, Maruyama Y, Ozawa K, Shibasaki J, Nishimura G, Kurosawa K. 2010. Prenatal findings of paternal uniparental disomy 14: Report of four patients. Am J Med Genet Part A 152A:789–791.

Journal of Human Genetics (2011) 56, 91–93

www.nature.com/jhg

SHORT COMMUNICATION

Androgenetic/biparental mosaicism in a girl with Beckwith–Wiedemann syndrome-like and upd(14)pat-like phenotypes

Kazuki Yamazawa[1,5], Kazuhiko Nakabayashi[2], Kentaro Matsuoka[3], Keiko Masubara[1], Kenichiro Hata[2], Reiko Horikawa[4] and Tsutomu Ogata[1]

This report describes androgenetic/biparental mosaicism in a 4-year-old Japanese girl with Beckwith–Wiedemann syndrome (BWS)-like and paternal uniparental disomy 14 (upd(14)pat)-like phenotypes. We performed methylation analysis for 18 differentially methylated regions on various chromosomes, genome-wide microsatellite analysis for a total of 90 loci and expression analysis of *SNRPN* in leukocytes. Consequently, she was found to have an androgenetic 46,XX cell lineage and a normal 46,XX cell lineage, with the frequency of the androgenetic cells being roughly calculated as 91% in leukocytes, 70% in tongue tissues and 79% in tonsil tissues. It is likely that, after a normal fertilization between an ovum and a sperm, the paternally derived pronucleus alone, but not the maternally derived pronucleus, underwent a mitotic division, resulting both in the generation of the androgenetic cell lineage by endoreplication of one blastomere containing a paternally derived pronucleus and in the formation of the normal cell lineage by union of paternally and maternally derived pronuclei. It appears that the extent of overall (epi)genetic aberrations exceeded the threshold level for the development of BWS-like and upd(14)pat-like phenotypes, but not for the occurrence of other imprinting disorders or recessive Mendelian disorders.
Journal of Human Genetics (2011) **56**, 91–93; doi:10.1038/jhg.2010.142; published online 11 November 2010

Keywords: androgenesis; Beckwith–Wiedemann syndrome; mosaicism; upd(14)pat

INTRODUCTION

A pure androgenetic human with paternal uniparental disomy for all chromosomes is incompatible with life because of genomic imprinting.[1,2] However, a human with an androgenetic cell lineage could be viable in the presence of a normal cell lineage. Indeed, an androgenetic cell lineage has been identified in six liveborn individuals with variable phenotypes.[3–7] All the androgenetic cell lineages have a 46,XX karyotype, and this is consistent with the lethality of an androgenetic 46,YY cell lineage.

Here, we report on a girl with androgenetic/biparental mosaicism, and discuss the underlying factors for the phenotypic development.

CASE REPORT

This patient was conceived naturally to non-consanguineous and healthy parents. At 24 weeks gestation, the mother was referred to us because of threatened premature delivery. Ultrasound studies showed Beckwith–Wiedemann syndrome (BWS)-like features,[8] such as macroglossia, organomegaly and umbilical hernia, together with polyhydramnios and placentomegaly. The mother repeatedly received amnioreduction and tocolysis.

She was delivered by an emergency cesarean section because of preterm rupture of membranes at 34 weeks of gestation. Her birth weight was 3730 g (+4.8 s.d. for gestational age), and her length 45.6 cm (+0.7 s.d.). The placenta weighed 1040 g (+7.3 s.d.).[9] She was admitted to a neonatal intensive care unit due to asphyxia. Physical examination confirmed a BWS-like phenotype. Notably, chest roentgenograms delineated mild bell-shaped thorax characteristic of paternal uniparental disomy 14 (upd(14)pat),[10] although coat hanger appearance of the ribs indicative of upd(14)pat was absent (Supplementary Figure 1). She was placed on mechanical ventilation for 2 months, and received tracheostomy, glossectomy and tonsillectomy in her infancy, due to upper airway obstruction. She also had several clinical features occasionally reported in BWS[8] (Supplementary Table 1). Her karyotype was 46,XX in all the 50 lymphocytes analyzed. On the last examination at 4 years of age, she showed postnatal growth failure and severe developmental retardation.

[1]Department of Molecular Endocrinology, National Research Institute for Child Health and Development, Tokyo, Japan; [2]Department of Maternal-Fetal Biology, National Research Institute for Child Health and Development, Tokyo, Japan; [3]Division of Pathology, National Medical Center for Children and Mothers, Tokyo, Japan and [4]Division of Endocrinology and Metabolism, National Medical Center for Children and Mothers, Tokyo, Japan
[5]Current address: Department of Physiology, Development & Neuroscience, University of Cambridge, Cambridge, UK.
Correspondence: Dr T Ogata, Department of Molecular Endocrinology, National Research Institute for Child Health and Development, 2-10-1 Ohkura, Setagaya, Tokyo 157-8535, Japan.
E-mail: tomogata@nch.go.jp
Received 9 September 2010; revised 18 October 2010; accepted 22 October 2010; published online 11 November 2010

MOLECULAR STUDIES

This study was approved by the Institutional Review Board Committee at the National Center for Child health and Development, and performed after obtaining informed consent.

Methylation analysis

We first performed bisulfite sequencing for the *H19*-DMR (differentially methylated region) and KvDMR1 as a screening of BWS[11,12] and that for the IG-DMR and the *MEG3*-DMR as a screening of upd(14)pat,[10] using leukocyte genomic DNA. Paternally derived clones were predominantly identified for the four DMRs examined (Figure 1a). We next performed combined bisulfite restriction analysis for multiple DMRs, as reported previously.[13] All the autosomal DMRs exhibited markedly skewed methylation patterns consistent with predominance of paternally inherited clones, whereas the *XIST*-DMR on the X chromosome showed a normal methylation pattern (Figure 1a).

Genome-wide microsatellite analysis

Microsatellite analysis was performed for 90 loci with high heterozygosities in the Japanese population.[14] Major peaks consistent with paternal uniparental isodisomy and minor peaks of maternal origin were identified for at least one locus on each chromosome, with the minor peaks of maternal origin being more obvious in tongue and tonsil tissues than in leukocytes (Figure 1b and Supplementary Table 2). There were no loci with three or four peaks indicative of chimerism. The frequency of the androgenetic cells was calculated as 91% in leukocytes, 70% in tongue cells and 79% in tonsil cells, although the estimation apparently was a rough one (for details, see Supplementary Methods).

Expression analysis

We examined *SNRPN* expression, because *SNRPN* showed strong expression in leukocytes (for details, see Supplementary Data). *SNRPN* expression was almost doubled in the leukocytes of this patient (Figure 1c).

DISCUSSION

These results suggest that this patient had an androgenetic 46,XX cell lineage and a normal 46,XX cell lineage. In this regard, both the androgenetic and the biparental cell lineages appear to have derived from a single sperm and a single ovum, because a single haploid genome of paternal origin and that of maternal origin were identified in this patient by genome-wide microsatellite analysis. Thus, it is likely that after a normal fertilization between an ovum and a sperm, the paternally derived pronucleus alone, but not the maternally derived pronucleus, underwent a mitotic division, resulting both in the generation of the androgenetic cell lineage by endoreplication of

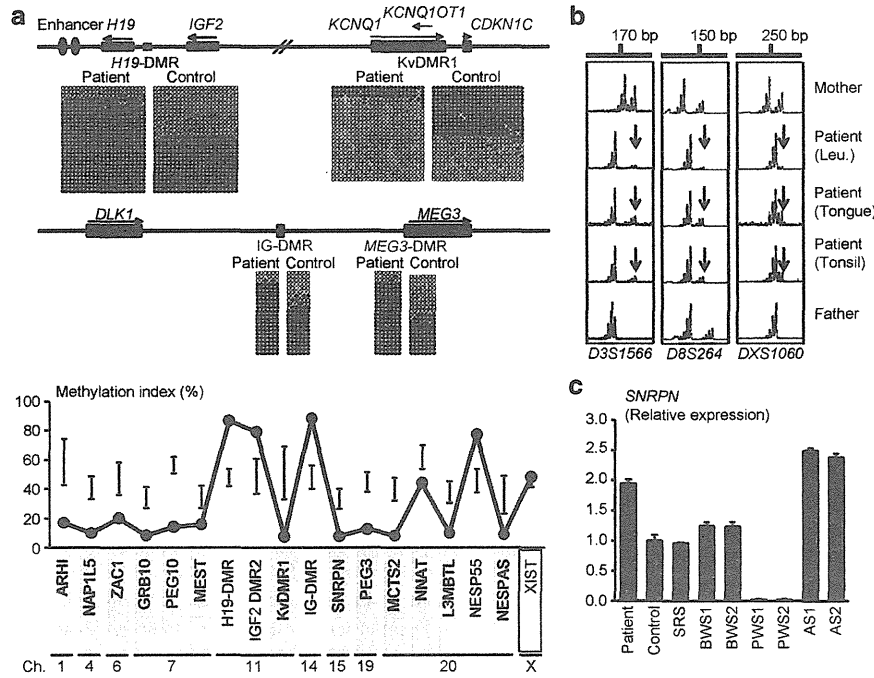

Figure 1 Representative molecular results. (**a**) Methylation analysis. Upper part: Bisulfite sequencing data for the *H19*-DMR and the KvDMR1 on 11p15.5, and those for the IG-DMR and the *MEG3*-DMR on 14q32.2. Each line indicates a single clone, and each circle denotes a CpG dinucleotide; filled and open circles represent methylated and unmethylated cytosines, respectively. Paternally expressed genes are shown in blue, maternally expressed gene in red, and the DMRs in green. The *H19*-DMR, the IG-DMR, and the *MEG3*-DMR are usually methylated after paternal transmission and unmethylated after maternal transmission, whereas the KvDMR1 is usually unmethylated after paternal transmission and methylated after maternal transmission.[10,11] Lower part: Methylation indices (the ratios of methylated clones) obtained from the COBRA analyses for the 18 DMRs. The DMRs highlighted in blue and pink are methylated after paternal and maternal transmissions, respectively. The black vertical bars indicate the reference data (maximum – minimum) in leukocyte genomic DNA of 20 normal control subjects (the *XIST*-DMR data are obtained from 16 control females). (**b**) Representative microsatellite analysis. Major peaks of paternal origin and minor peaks of maternal origin (red arrows) have been identified in this patient. The minor peaks of maternal origin are more obvious in tongue and tonsil tissues than in leukocytes (Leu.). (**c**) Relative expression level (mean ± s.d.) of *SNRPN*. The data are normalized against *TBP*. SRS: an SRS patient with an epimutation (hypomethylation) of the *H19*-DMR; BWS1: a BWS patient with an epimutation (hypermethylation) of the *H19*-DMR; BWS2: a BWS patient with upd(11)pat; PWS1: a Prader-Willi syndrome (PWS) patient with upd(15)mat; PWS2: a PWS patient with an epimutation (hypermethylation) of the *SNRPN*-DMR; AS1: an Angelman syndrome (AS) patient with upd(15)pat; and AS2: an AS patient with an epimutation (hypomethylation) of the *SNRPN*-DMR. The data were obtained using an ABI Prism 7000 Sequence Detection System (Applied Biosystems).

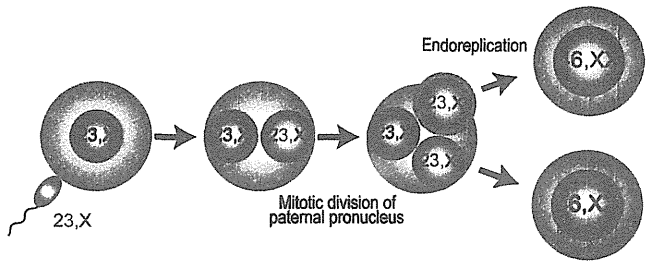

Figure 2 Schematic representation of the generation of the androgenetic/biparental mosaicism. Polar bodies are not shown.

one blastomere containing a paternally derived pronucleus and in the formation of the normal cell lineage by union of paternally and maternally derived pronuclei (Figure 2). This model has been proposed for androgenetic/biparental mosaicism generated after fertilization between a single ovum and a single sperm.[5,15,16] The normal methylation pattern of the *XIST*-DMR is explained by assuming that the two X chromosomes in the androgenetic cell lineage undergo random X-inactivation, as in the normal cell lineage. Furthermore, the results of microsatellite analysis imply that the androgenetic cells were more prevalent in leukocytes than in tongue and tonsil tissues.

A somatic androgenetic cell lineage has been identified in seven liveborn patients including this patient (Supplementary Table 1).[3–7] In this context, leukocytes are preferentially utilized for genetic analyses in human patients, and detailed examinations such as analyses of plural DMRs are necessary to detect an androgenetic cell lineage. Thus, the hitherto identified patients would be limited to those who had androgenetic cells as a predominant cell lineage in leukocytes probably because of a stochastic event and received detailed molecular studies. If so, an androgenetic cell lineage may not be so rare, and could be revealed by detailed analyses as well as examinations of additional tissues in patients with relatively complex phenotypes, as observed in the present patient.

Phenotypic features in androgenetic/biparental mosaicism would be determined by several factors. They include (1) the ratio of two cell lineages in various tissues/organs, (2) the number of imprinted domains relevant to specific features (for example, dysregulation of the imprinted domains on 11p15.5 and 14q32.2 is involved in placentomegaly[9,17]), (3) the degree of clinical effects of dysregulated imprinted domains (an (epi)dominant effect has been assumed for the 11p15.5 imprinted domains[18]), (4) expression levels of imprinted genes in androgenetic cells (although *SNRPN* expression of this patient was consistent with androgenetic cells being predominant in leukocytes, complicated expression patterns have been identified for several imprinted genes in both androgenetic and parthenogenetic fetal mice, probably because of perturbed *cis*- and *trans*-acting regulatory mechanisms[19]) and (5) unmasking of possible paternally inherited recessive mutation(s) in androgenetic cells. Thus, in this patient, it appears that the extent of overall (epi)genetic aberrations exceeded the threshold level for the development of BWS-like and upd(14)pat-like body and placental phenotypes, but remained below the threshold level for the occurrence of other imprinting disorders or recessive Mendelian disorders.

CONFLICT OF INTEREST

The authors declare no conflict of interest.

ACKNOWLEDGEMENTS

This work was supported by grants from the Ministry of Health, Labor, and Welfare, and the Ministry of Education, Science, Sports and Culture.

1 Surani, M. A., Barton, S. C. & Norris, M. L. Development of reconstituted mouse eggs suggests imprinting of the genome during gametogenesis. *Nature* **308,** 548–550 (1984).
2 McGrath, J. & Solter, D. Completion of mouse embryogenesis requires both the maternal and paternal genomes. *Cell* **37,** 179–183 (1984).
3 Hoban, P. R., Heighway, J., White, G. R., Baker, B., Gardner, J., Birch, J. M. *et al.* Genome-wide loss of maternal alleles in a nephrogenic rest and Wilms' tumour from a BWS patient. *Hum. Genet.* **95,** 651–656 (1995).
4 Bryke, C. R., Garber, A. T. & Israel, J. Evolution of a complex phenotype in a unique patient with a paternal uniparental disomy for every chromosome cell line and a normal biparental inheritance cell line. *Am. J. Hum. Genet.* **75**(Suppl), 831 (2004).
5 Giurgea, I., Sanlaville, D., Fournet, J. C., Sempoux, C., Bellanne-Chantelot, C. & Touati, G. Congenital hyperinsulinism and mosaic abnormalities of the ploidy. *J. Med. Genet.* **43,** 248–254 (2006).
6 Wilson, M., Peters, G., Bennetts, B., McGillivray, G., Wu, Z. H., Poon, C. *et al.* The clinical phenotype of mosaicism for genome-wide paternal uniparental disomy: two new reports. *Am. J. Med. Genet. Part A* **146A,** 137–148 (2008).
7 Reed, R. C., Beischel, L., Schoof, J., Johnson, J., Raff, M. L. & Kapur, R. P. Androgenetic/biparental mosaicism in an infant with hepatic mesenchymal hamartoma and placental mesenchymal dysplasia. *Pediatr. Dev. Pathol.* **11,** 377–383 (2008).
8 Jones, K. L. *Smith's Recognizable Patterns of Human Malformation* 6th edn. (Elsevier Saunders: Philadelphia, 2006).
9 Kagami, M., Yamazawa, K., Matsubara, K., Matsuo, N. & Ogata, T. Placentomegaly in paternal uniparental disomy for human chromosome 14. *Placenta* **29,** 760–761 (2008).
10 Kagami, M., Sekita, Y., Nishimura, G., Irie, M., Kato, F., Okada, M. *et al.* Deletions and epimutations affecting the human 14q32.2 imprinted region in individuals with paternal and maternal upd(14)-like phenotypes. *Nat. Genet.* **40,** 237–242 (2008).
11 Yamazawa, K., Kagami, M., Nagai, T., Kondoh, T., Onigata, K., Maeyama, K. *et al.* Molecular and clinical findings and their correlations in Silver-Russell syndrome: implications for a positive role of IGF2 in growth determination and differential imprinting regulation of the IGF2-H19 domain in bodies and placentas. *J. Mol. Med.* **86,** 1171–1181 (2008).
12 Weksberg, R., Shuman, C. & Beckwith, J. B. Beckwith-Wiedemann syndrome. *Eur. J. Hum. Genet.* **18,** 8–14 (2010).
13 Yamazawa, K., Nakabayashi, K., Kagami, M., Sato, T., Saitoh, S., Horikawa, R. *et al.* Parthenogenetic chimaerism/mosaicism with a Silver-Russell syndrome-like phenotype. *J. Med. Genet.* **47,** 782–785 (2010).
14 Ikari, K., Onda, H., Furushima, K., Maeda, S., Harata, S. & Takeda, J. Establishment of an optimized set of 406 microsatellite markers covering the whole genome for the Japanese population. *J. Hum. Genet.* **46,** 207–210 (2001).
15 Kaiser-Rogers, K. A., McFadden, D. E., Livasy, C. A., Dansereau, J., Jiang, R., Knops, J. F. *et al.* Androgenetic/biparental mosaicism causes placental mesenchymal dysplasia. *J. Med. Genet.* **43,** 187–192 (2006).
16 Kotzot, D. Complex and segmental uniparental disomy updated. *J. Med. Genet.* **45,** 545–556 (2008).
17 Monk, D., Arnaud, P., Apostolidou, S., Hills, F. A., Kelsey, G., Stanier, P. *et al.* Limited evolutionary conservation of imprinting in the human placenta. *Proc. Natl. Acad. Sci. USA.* **103,** 6623–6628 (2006).
18 Azzi, S., Rossignol, S., Steunou, V., Sas, T., Thibaud, N., Danton, F. *et al.* Multilocus methylation analysis in a large cohort of 11p15-related foetal growth disorders (Russell Silver and Beckwith Wiedemann syndromes) reveals simultaneous loss of methylation at paternal and maternal imprinted loci. *Hum. Mol. Genet.* **18,** 4724–4733 (2009).
19 Ogawa, H., Wu, Q., Komiyama, J., Obata, Y. & Kono, T. Disruption of parental-specific expression of imprinted genes in uniparental fetuses. *FEBS Lett.* **580,** 5377–5384 (2006).

Supplementary Information accompanies the paper on Journal of Human Genetics website (http://www.nature.com/jhg)

Journal of Human Genetics (2011) 56, 94–96

www.nature.com/jhg

SHORT COMMUNICATION

Low prevalence of classical galactosemia in Korean population

Beom Hee Lee[1,2,3,6], Chong Kun Cheon[4,6], Jae-Min Kim[2], Minji Kang[2], Joo Hyun Kim[2], Song Hyun Yang[5], Gu-Hwan Kim[2,3], Jin-ho Choi[1] and Han-Wook Yoo[1,2,3]

This study described the clinical and molecular genetic features of classical galactosemia in Korean population to contribute to the insight in the spectrum of galactosemia in the world, as little is known about the spectrum and incidence of galactosemia in Asia. During the 11-year study period, only three Korean children were identified as having classical galactosemia on the basis of the enzymatic and molecular genetic analysis. Asians have been reported to have mutations distinct from those of Caucasians and African Americans, indicating that galactose-1-phosphate uridyltransferase mutations are ethnically diverse. Our three patients had a total of three mutations (c.252+1G>A, p.Q169H and p.E363K), two of which were novel (p.E363K and c.252+1G>A) mutations. Interestingly, c.252+1G>A, which leads to skipping of exon 2, was observed in all three patients (three of six alleles), indicating that this mutation may be common in Koreans with classical galactosemia. Screening for classical galactosemia in 158 126 Korean newborns identified no patient with classical galactosemia. In conclusion, our findings provide further evidence for the ethnic diversity of classical galactosemia, which may be as rare in Koreans as in other Asian populations.

Journal of Human Genetics (2011) **56**, 94–96; doi:10.1038/jhg.2010.152; published online 9 December 2010

Keywords: ethnic divergence; galactosemia; GALT; mutation

Classical galactosemia (OMIM 230400) is caused by a deficiency in galactose-1-phosphate uridyltransferase (GALT; EC2.7.712). Classical galactosemia is characterized by more severe clinical manifestations than the other two types, galactosemia II or III, with newborns usually manifesting symptoms within a few days of birth after milk feeding.[1–3]

The incidence of classical galactosemia in western Europe has been estimated to be between 1:23 000 and 1:89 000.[1,4,5] In Korean newborns, the overall incidence of the three types of galactosemia have been reported to be approximately 1:40 000,[6] but the exact incidence of classical galactosemia is not yet known. Since the first report of a mutation in the *GALT* gene,[7] more than 200 different mutations have been identified with missense mutations being observed most commonly (http://www.hgmd.org).[1,8] The most common mutations in Caucasian and African American populations are p.Q188R and p.S135L, respectively,[9–11] but neither of these mutations have been detected to date in Asian populations. Similarly, Japanese patients have distinct mutations, such as p.V85_N97delinsRfsX8, p.W249X and p.R231H, which have not been observed in Caucasians and African Americans, providing further evidence for genetic heterogeneities among ethnic groups.[1,12,13]

Between March 1999 and May 2010, only three unrelated Korean patients were diagnosed with classical galactosemia at the Asan Medical Center, Seoul, Korea, with the diagnosis of each confirmed by enzyme assays and molecular genetic analysis (Table 1). All patients were identified by neonatal screening program performed at 3–5 days of life. Patients 1 and 2 had neonatal jaundice with slightly increased serum hepatic enzyme concentrations, which was not progressive, whereas patient 3 had clinically deteriorated and showed progressive jaundice and a bleeding tendency, while awaiting the results of screening tests that were reported on the eleventh day after birth (Table 1). Median total plasma galactose concentration was 50 mg per 100 ml (range, 13.5–68.9 mg per 100 ml; normal range <13 mg per 100 ml) and median erythrocyte galactose-1-phosphate concentration was 10.4 mg per 100 ml (range 1.60–62.8 mg per 100 ml; normal range <0.3 mg per 100 ml). The GALT activity was decreased in all patients, ranging from 0.1 to 0.8 umol hr^{-1} per gram hemoglobin (median, 0.3umol hr^{-1} per gram hemoglobin; normal range, 25.7 ± 3.6 umol hr^{-1} per gram hemoglobin) (Table 1). A galactose-restricted diet was effective in decreasing galactose and galactose-1-phosphate concentrations in all patients. The hepatic dysfunction, jaundice and

[1]Department of Pediatrics, Asan Medical Center Children's Hospital, University of Ulsan College of Medicine, Seoul, Korea; [2]Genome Research Center for Birth defects and Genetic Diseases, Asan Medical Center Children's Hospital, University of Ulsan College of Medicine, Seoul, Korea; [3]Medical Genetics Clinic and Laboratory, Asan Medical Center Children's Hospital, University of Ulsan College of Medicine, Seoul, Korea; [4]Department of Pediatrics, Genetic and Metabolic Clinic, Children Hospital, Pusan National University, Gyeongnam, South Korea and [5]Green Cross Reference Laboratory, Seoul, Korea
[6]These authors contributed equally to this paper as first authors.
Correspondence: Dr H-W Yoo, Genome Research Center for Birth defects and Genetic Diseases, Asan Medical Center Children's Hospital, University of Ulsan College of Medicine, 388-1 Pungnap-Dong, Songpa-Gu, Seoul 138-736, Korea.
E-mail: hwyoo@amc.seoul.kr
Received 13 September 2010; revised 14 October 2010; accepted 9 November 2010; published online 9 December 2010

Molecular Genetics and Metabolism 100 (2010) 269–273

Contents lists available at ScienceDirect

Molecular Genetics and Metabolism

journal homepage: www.elsevier.com/locate/ymgme

Anorectal and urinary anomalies and aberrant retinoic acid metabolism in cytochrome P450 oxidoreductase deficiency

Maki Fukami [a,*], Toshiro Nagai [b], Hiroshi Mochizuki [c], Koji Muroya [d], Gen Yamada [e], Kimitaka Takitani [f], Tsutomu Ogata [a]

[a] Department of Endocrinology and Metabolism, National Research Institute for Child Health and Development, Tokyo, Japan
[b] Department of Pediatrics, Dokkyo Medical University Koshigaya Hospital, Koshigaya, Japan
[c] Department of Endocrinology and Metabolism, Saitama Children's Medical Center, Saitama, Japan
[d] Division of Endocrinology and Metabolism, Kanagawa Children's Medical Center, Yokohama, Japan
[e] Institute of Molecular Embryology and Genetics, Kumamoto University, Kumamoto, Japan
[f] Department of Pediatrics, Osaka Medical College, Osaka, Japan

ARTICLE INFO

Article history:
Received 29 January 2010
Received in revised form 31 March 2010
Accepted 31 March 2010
Available online 3 April 2010

Keywords:
Cytochrome P450 oxidoreductase
POR
CYP26
Retinoic acid
Imperforate anus
Vesicoureteral reflux

ABSTRACT

Context: Cytochrome P450 oxidoreductase (POR) is an electron donor for all microsomal P450 enzymes including CYP26 involved in inactivation of all-trans retinoic acid (atRA). Although previous studies in *Por* knockout mice suggest that atRA accumulation is relevant to various posterior organ abnormalities, a systematic analysis has not been performed for anorectal and urinary anomalies in patients with POR deficiency (PORD).

Objective: To report the frequencies of anorectal and urinary anomalies and plasma atRA values in PORD patients.

Patients: We studied 37 Japanese patients with PORD, consisting of 15 homozygotes for R457H (group A), 15 compound heterozygotes for R457H and one apparently null mutation (group B), and seven patients with other combinations of mutations (group C). Since R457H is a severe hypomorphic mutation, the residual POR function is predicted to be higher in group A than in group B.

Results: Imperforate anus was observed in four patients (10.8%) and vesicoureteral reflux was found in three patients (8.1%), with no significant difference in the frequencies of such anomalies between groups A and B. In addition, a complex urogenital malformation including penile agenesis was identified in one patient. Plasma atRA values were above the reference range in nine of 12 patients examined, and were similar between groups A and B and between patients with and without anomalies.

Conclusions: The results imply that aberrant atRA metabolism due to CYP26 deficiency underlies various anorectal and urinary anomalies in patients with PORD. Clinical phenotypes may be primarily determined by maternal oral retinol intake during pregnancy, and plasma atRA values may be largely influenced by the amount of postnatal oral retinol intake in such patients.

Introduction

Cytochrome P450 oxidoreductase (POR) is an electron donor for all microsomal cytochrome P450 enzymes and several non-P450 microsomal enzymes [1]. Molecular abnormalities of *POR* lead to an autosomal recessive disorder characterized by skeletal dysplasia referred to as Antley–Bixler syndrome, adrenal dysfunction, 46,XX and 46,XY disorders of sex development (DSD), and maternal virilization during pregnancy [2,3]. Of these salient clinical features, skeletal dysplasia is primarily ascribed to impaired activities of POR-dependent cholesterolgenic enzymes CYP51A1 (lanosterol 14α-demethylase) and SQLE (squalene monooxygenase) in bone tissues, and the remaining features are primarily caused by defective activities of POR-dependent steroidogenic enzymes CYP17A1 (17α-hydroxylase and 17,20 lyase), CYP21A2 (21-hydroxylase), and CYP19A1 (aromatase) in adrenals, gonads, and placenta [3]. In addition, the backdoor pathway to dihydrotestosterone, which appears to take place in fetal adrenals, also plays a pivotal role in the development of 46,XX DSD [3,4]. Since all patients reported to date have at least one missense mutation with probable residual

Abbreviations: atRA, all-trans retinoic acid; IA, imperforate anus; POR, cytochrome P450 oxidoreductase; DSD, disorders of sex development; SQLE, squalene monooxigenase; RA, retinoic acid; RALDH, retinal dehydrogenase; PORD, POR deficiency; UTI, urinary tract infection; VUR, vesicoureteral reflux.

* Corresponding author. Address: Department of Endocrinology and Metabolism, National Research Institute for Child Health and Development, 2-10-1 Ohkura, Setagaya, Tokyo 157-8535, Japan. Fax: +81 3 5494 7026.
E-mail address: mfukami@nch.go.jp (M. Fukami).

1096-7192/$ - see front matter © 2010 Elsevier Inc. All rights reserved.
doi:10.1016/j.ymgme.2010.03.023

functions, this suggests that complete loss of POR function is incompatible with life [3,4].

Retinoic acid (RA) is a signaling molecule involved in cell proliferation, differentiation, and apoptosis [5]. In human and murine fetuses, the most active form of RA, all-trans RA (atRA), is synthesized from maternally derived retinol by retinal dehydrogenase 2 (RALDH2/Raldh2) and retinol dehydrogenases, and converted into biologically inactive metabolites by CYP26/Cyp26 enzymes (primarily by CYP26A1/Cyp26a1 and partly by CYP26B1/Cyp26b1 and CYP26C1/Cyp26c1) [5–7]. The tissue concentration of atRA is tightly regulated by the balance between synthesis and inactivation, and both accumulation and deficiency of atRA lead to developmental defects [5,6]. Notably, murine embryos exposed to high-dose of atRA and those with a targeted deletion of *Cyp26a1* (*Cyp26a1*$^{-/-}$) manifest severe anomalies particularly in the hindgut, genital tubercle, and sacral/caudal vertebrae [8–10], indicating that posterior organs are highly susceptible to excessive atRA signaling.

Biological activities of CYP26 enzymes are supported by POR. Thus, it is predicted that POR deficiency (PORD) results in atRA accumulation because of impaired activities of CYP26 enzymes, leading to posterior organ anomalies. In support of this, *Por* knockout mice (*Por*$^{-/-}$), which are embryonic lethal, manifest severe posterior region anomalies comparable to those of *Cyp26a1*$^{-/-}$ mice [11]. Furthermore, previous studies have revealed that abnormal RA signaling takes place in the anorectal and urinary regions of *Por*$^{-/-}$ mouse embryos, and that phenotypes of these embryos are partially rescued by targeted deletion of *Raldh2* or by culturing the embryos in the serum-free medium (thus, retinol-free medium) [11]. These results imply that accumulation of atRA is involved in the development of posterior region abnormalities in *Por*$^{-/-}$ mice.

At present, however, a systematic phenotypic analysis has not been performed for posterior organ anomalies in PORD patients, although such anomalies have been described in a few of PORD patients [12,13]. Thus, we investigated anorectal and urinary anomalies and plasma atRA values in PORD patients.

Patients and methods

Patients

This study was approved by the Institutional Review Board Committee at National Center for Child Health and Development, and performed after obtaining written informed consent. We studied 37 Japanese patients with molecularly confirmed *POR* abnormalities (16 with 46,XY and 21 with 46,XX). Of the 37 patients, 35 have been reported previously [4]. The patients were classified into three groups on the basis of the mutation types: group A, homozygotes for the Japanese founder mutation R457H ($n = 15$); group B, compound heterozygotes for R457H and one apparently null mutation ($n = 15$); and group C, compound heterozygotes for other types of mutations ($n = 7$). Since R457H is a severe hypomorphic mutation with a low enzymatic activity [12], POR residual activity is predicted to be higher in group A than in group B, while it is unknown for group C.

Clinical assessment

Imperforate anus (IA) was evaluated by physical examination. Urinary anomalies such as vesicoureteral reflux (VUR) were assessed in patients with an episode(s) of urinary tract infection (UTI) by radiological studies including voiding cystourethrography and intravenous pyelography.

Measurement of plasma atRA values

Plasma atRA value was obtained by the previously described method [14]. In brief, a 2.5-ml aliquot of 0.1 ml phosphate buffer (pH 6.0) and 5 ml of ethyl ether were added to 1 ml of plasma. The mixture was vortexed and centrifuged at 3000 rpm for 15 min. A 4-ml aliquot of the upper layer was removed and evaporated to dryness, after which the residue was dissolved in methanol and analyzed by high-performance liquid chromatography using Nano-Space SI-2 pump (Shiseido, Tokyo) and a Capcell Pack-C18 UG120 column (Shiseido, Tokyo). The mobile phase consisted of 60% acetonitrile and 40% ammonium acetate buffer (v/v, 10%) at a flow rate of 1.5 ml/min. The samples were monitored using SPD-10A (Shimazu, Kyoto) with detection at 340 nm. The retention time of atRA was 7.5 min. Plasma atRA values of the patients were compared with reference values reported by Tang et al. [15].

Sequence analysis of HOX9–13 paralogs

To examine possible relevance of an additional gene mutation(s) in a patient with a complex phenotype including penile agenesis, we analyzed *HOX9–13* paralogs that are known to play a critical role in the urogenital and limb development [16]. In brief, leukocyte genomic DNA was PCR-amplified for all the coding exons and their flanking splice sites of *HOX9–13* paralogs, which are devoid of *HOXA12* and *HOXB10–12*, using the previously reported primers [17]. Subsequently, the PCR products were subjected to direct sequencing on a CEQ 8000 autosequencer (Beckman Coulter, Fullerton, CA). When a substitution was identified, the corresponding sequence was studied in the parents and 100 control subjects.

Statistical analysis

The statistical significance of the mean was analyzed by the *t*-test, and that of the frequency was examined by the χ^2 test. $P < 0.05$ was considered significant.

Results

Anorectal and/or urinary anomalies

IA was observed in two patients of group A, one patient of group B, and one patient of group C, and VUR was found in one patient of each group (Table 1). There was no significant difference in the frequencies of IA and VUR between group A with two copies of R457H and group B with a single copy of R457H ($P = 0.60$ for IA and $P = 1.00$ for VUR). In addition, a complex urogenital malformation including penile agenesis, aplasia of the left kidney, duplication and malrotation of the right kidney, and VUR was identified in one patient of group B (case 10) (Fig. 1). There were no other clinically discernible anorectal or urinary anomalies.

Plasma atRA values

Plasma atRA was obtained in three patients of group A, seven patients of group B, and two patients of group C (Table 1). Plasma atRA values were above the reference range in nine patients and remained within the reference range in three patients. There was no significant difference in the atRA values between groups A and B (2.3 ± 0.3 ng/ml vs. 2.1 ± 0.4 ng/ml, $P = 0.45$) and between patients with and without anorectal and/or renal anomalies (1.8 ± 0.2 ng/ml vs. 2.5 ± 0.6 ng/ml, $P = 0.07$).

Sequence analysis of HOX9–13 paralogs in case 10

A novel heterozygous missense substitution (G3A) was identified for *HOXD13*. This substitution was found in a phenotypically normal father as well as in three of 100 control subjects. No other

Table 1
Anorectal/urinary anomalies and plasma atRA values in PORD patients.

Patients			*POR* mutations	Anorectal and urinary anomalies	Plasma atRA values (ng/ml)
Case	Karyotype	Age (y)	Amino acid changes		
Group A: Homozygotes for R457H					
1	46,XY	2.0	R457H/R457H	IA	N.M.
2	46,XX	0.4	R457H/R457H	Absent	N.M.
3	46,XX	14.1	R457H/R457H	Absent	**2.5**
4	46,XX	15.0	R457H/R457H	VUR (B)	**1.9**
5	46,XX	3.0	R457H/R457H	Absent	**2.5**
6	46,XX	0.1	R457H/R457H	IA	N.M.
Group B: Compound heterozygotes for R457H and an apparently null mutation					
7	46,XY	16.8	R457H/Q201X	Absent	**2.5**
8	46,XY	14.8	R457H/I444fsX449	Absent	**2.4**
9	46,XY	17.5	R457H/transcription failure	Absent	**1.9**
10	46,XY	2.1	R457H/R48fsX63	Complex[a]	1.5
11	46,XY	0.2	R457H/Q555fsX612	Absent	**2.6**
12	46,XX	9.0	R457H/IVS6+1G>A	Absent	1.6
13	46,XX	6.6	R457H/transcription failure	VUR (R)	**2.0**
14	46,XX	4.2	R457H/transcription failure	IA	N.M.
Group C: Other compound heterozygotes					
15	46,XY	0.4	R457H/A462-S463insIA	Absent	**3.7**
16	46,XY	18.0	R457H/L612-W620delinsR	VUR (R)	N.M.
17	46,XX	0.8	R457H/E580Q	Absent	N.M.
18	46,XX	0.7	R457H/348delV	IA	1.8

The values above the reference range are boldfaced.
Of 37 patients with PORD, 19 patients are not included in this table, because they had no anorectal or urinary anomalies and were not examined for plasma atRA values.
POR, cytochrome P450 oxidoreductase; atRA, all-trans retinoic acid; IA, imperforate anus; VUR, vesicoureteral reflux; R, right; B, bilateral; N.M., not measured.
Reference values: 1.0–1.8 ng/ml for atRA.
[a] Renal aplasia (L), renal duplication (R), renal malrotation, VUR (B), and penile agenesis.

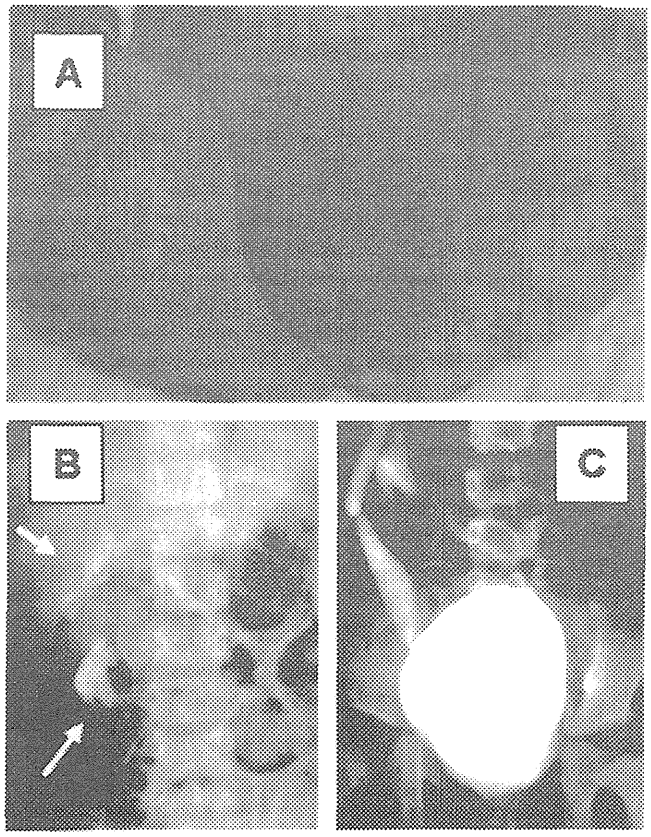

Fig. 1. Clinical phenotypes in case 10. (A) Penile agenesis. (B) Intravenous pyelography delineating aplasia of the left kidney and duplication and malrotation of the right kidney (arrows). (C) Voiding cystourethrography showing severe VUR.

sequence substitution was detected for the *HOX9–13* paralogs examined.

Discussion

We studied 37 patients with PORD and identified IA in four patients and VUR in three patients, as well as a complex urogenital malformation in a single patient. The frequencies of IA and VUR are obviously higher in PORD patients (10.8% for IA and 8.1% for VUR) than in the normal population (~0.0002% for IA and ~1.0% for VUR) [18,19]. In addition, the prevalence of VUR in the PORD patients may have been underestimated, because detailed urinary studies were carried out only in patients with an episode(s) of UTI. Thus, these findings imply that anorectal and urinary anomalies are characteristic features in PORD.

However, the frequencies of anorectal and urinary anomalies remained low, compared to those of salient clinical features such as skeletal dysplasia, adrenal dysfunction, DSD, and maternal virilization during pregnancy [4]. This suggests that a relatively low residual POR activity can permit normal anorectal and urinary development. Consistent with this, mice with a partial *Por* deletion that retains some residual activity lack anorectal and urinary anomalies, although they manifest severe limb defects [20]. Thus, PORD may function as a susceptibility or contributing factor, rather than a determinative factor, for the development of anorectal and urinary anomalies.

Plasma atRA values were elevated in most patients with PORD. This is compatible with reduced supporting activity of POR for CYP26 enzymes. Since plasma atRA is derived from specific atRA-producing tissues including liver and anorectal and urinary tissues [5], the atRA concentration may be drastically increased in such tissues. In this context, it is known that atRA functions as a paracrine or autocrine signaling factor [5] and regulates cellular apoptosis of the developing hindgut and the ureteric buds that are required for the normal anorectal and urinary development [21,22]. Thus, anorectal and urinary anomalies in PORD patients would primarily be ascribed to impaired CYP26 enzyme activities and resultant atRA accumulation in the anorectal and urinary regions. Indeed, liver-specific *Por* knockout mice have no discernible

abnormalities in the extra-hepatic organs including caudal regions, despite probably increased plasma atRA values because of impaired atRA inactivation in the liver [23].

Anorectal and urinary anomalies were identified in groups A–C with no difference in the prevalence between groups A and B, and plasma atRA values were similar between groups A and B and between patients with and without anorectal and urinary anomalies. In this regard, anorectal and urinary anomalies are generated in fetal life, and previous studies have indicated that phenotypic severity of *Por*$^{-/-}$, *Cyp26a1c1*$^{-/-}$, and *Cyp26a1b1c1*$^{-/-}$ mice embryos are obviously mitigated by a vitamin A-deficient diet and worsened by administration of a small dose of atRA during pregnancy [24,25]. Thus, while oral atRA intake would be neglectable in the daily human life, anorectal and urinary phenotypes in PORD patients may largely be influenced by the amount of maternal oral retinol intake during pregnancy. In addition, plasma atRA values in PORD patients would be influenced by the amount of postnatal oral retinol intake in such patients and would not reflect the amount of retinol transferred to such patients during pregnancy. These notions would explain the lack of correlation between the frequency of anomalies, postnatal plasma atRA values, and residual POR activities, although genetic factors such as polymorphisms of genes encoding atRA-synthesizing enzymes and/or RA binding protein would also be relevant to the variations in clinical phenotypes and plasma atRA values in PORD patients. Thus, it would be recommended to avoid retinol-rich foods during pregnancy of fetuses with a possibility of PORD.

A complex urogenital anomaly was identified in case 10. This phenotype may be explained as an extremely severe phenotype in PORD. In support of this, exposure to a large amount of retinol during pregnancy has caused renal and penile agenesis in a human patient [26]. Alternatively, there may be a hidden mutation(s) or susceptibility factor(s) in case 10, although we did not identify a definitive mutation in *HOX9–13* paralogs involved in the urogenital and limb development [16].

Several points should be made with respect to the present study. First, although a comprehensive skeletal survey was not performed in this study, impaired CYP26 activities in PORD may also lead to skeletal anomalies in the posterior region. Indeed, hemivertebrae and vertebral homeotic transformation have previously been identified in two PORD patients [12], and *Cyp26a1*$^{-/-}$ mice frequently exhibit vertebral anomalies such as spina bifida [9]. Second, impaired activities of POR-dependent enzymes other than CYP26 enzymes may also be relevant to anorectal and urinary anomalies. Indeed, reduced CYP51A1 and SQLE activities may affect the expression of several genes including *BMP4* and *FGF8* involved in posterior organ formation [27], because of intracellular cholesterol deficiency and resultant abnormal hedgehog signaling [28]. In support of this, Smith–Lemli–Opitz syndrome caused by mutations of *DHCR7* involved in cholesterolgenesis is often associated with Hirschsprung disease and renal malformations [29]. Lastly, while R457H is the most prevalent founder mutation in Japanese patients [4], A287P is the most common mutation in Caucasian patients [3,12]. In this context, supporting activities for POR-dependent steroidogenic enzymes are more severely compromised in R457H than in A287P [12] and, consistent with this, salient PORD phenotypes appear to be more severe in Japanese patients than in Caucasian patients [4,12]. Thus, while IA has also been identified in a Caucasian patient with A287P [12], the prevalence and the severity of anorectal and urinary anomalies remain to be clarified in different ethnic groups including Caucasian population.

In summary, the present study suggests that aberrant atRA metabolism due to CYP26 deficiency underlies anorectal and urinary anomalies in patients with PORD. Further studies will permit to define phenotypic spectrum in PORD and underlying factors for the development of clinical features.

Disclosure statement

The authors have nothing to declare.

Acknowledgments

We thank Drs. K. Hanaki, A. Uematsu, T. Ishii, C. Numakura, H. Sawada, M. Nakacho, T. Kowase, K. Motomura, H. Haruna, M. Nakamura, A. Ohishi, M. Adachi, T. Tajima, Y. Hasegawa, T. Hasegawa, R. Horikawa, T. Ohashi, R. Takeda, and I. Fujiwara for providing us with clinical data and blood samples of the patients. We also thank Drs. G. Nishimura and K. Homma for screening analysis of the patients. This study was supported by grants from the Ministry of Health, Labor, and Welfare and from the Ministry of Education, Culture, Sports, Science, and Technology.

References

[1] M. Wang, D.L. Roberts, R. Paschke, T.M. Shea, B.S. Masters, J.J. Kim, Three-dimensional structure of NADPH–cytochrome P450 reductase: prototype for FMN- and FAD-containing enzymes, Proc. Natl. Acad. Sci. USA 94 (1997) 8411–8416.
[2] C.E. Flück, T. Tajima, A.V. Pandey, W. Arlt, K. Okuhara, C.F. Verge, E.W. Jabs, B.B. Mendonça, K. Fujieda, W.L. Miller, Mutant P450 oxidoreductase causes disordered steroidogenesis with and without Antley–Bixler syndrome, Nat. Genet. 36 (2004) 228–230.
[3] R.R. Scott, W.L. Miller, Genetic and clinical features of P450 oxidoreductase deficiency, Horm. Res. 69 (2008) 266–275.
[4] M. Fukami, G. Nishimura, K. Homma, T. Nagai, K. Hanaki, A. Uematsu, T. Ishii, C. Numakura, H. Sawada, M. Nakacho, T. Kowase, K. Motomura, H. Haruna, M. Nakamura, A. Ohishi, M. Adachi, T. Tajima, Y. Hasegawa, T. Hasegawa, R. Horikawa, K. Fujieda, T. Ogata, Cytochrome P450 oxidoreductase deficiency: identification and characterization of biallelic mutations and genotype–phenotype correlations in 35 Japanese patients, J. Clin. Endocrinol. Metab. 94 (2009) 1723–1731.
[5] G. Duester, Retinoic acid synthesis and signaling during early organogenesis, Cell 134 (2008) 921–931.
[6] S. Abu-Abed, P. Dollé, D. Metzger, B. Beckett, P. Chambon, M. Petkovich, The retinoic acid-metabolizing enzyme, CYP26A1, is essential for normal hindbrain patterning, vertebral identity, and development of posterior structures, Genes Dev. 15 (2001) 226–240.
[7] M. Taimi, C. Helvig, J. Wisniewski, H. Ramshaw, J. White, M. Amad, B. Korczak, M. Petkovich, A novel human cytochrome P450, CYP26C1, involved in metabolism of 9-cis and all-trans isomers of retinoic acid, J. Biol. Chem. 279 (2004) 77–85.
[8] Y. Sasaki, N. Iwai, T. Tsuda, O. Kimura, Sonic hedgehog and bone morphogenetic protein 4 expressions in the hindgut region of murine embryos with anorectal malformations, Pediatr. Surg. 39 (2004) 170–173.
[9] K. Niederreither, S. Abu-Abed, B. Schuhbaur, M. Petkovich, P. Chambon, P. Dollé, Genetic evidence that oxidative derivatives of retinoic acid are not involved in retinoid signaling during mouse development, Nat. Genet. 31 (2002) 84–88.
[10] Y. Sakai, C. Meno, H. Fujii, J. Nishino, H. Shiratori, Y. Saijoh, J. Rossant, H. Hamada, The retinoic acid-inactivating enzyme CYP26 is essential for establishing an uneven distribution of retinoic acid along the anterio-posterior axis within the mouse embryo, Genes Dev. 15 (2001) 213–225.
[11] V. Ribes, D.M. Otto, L. Dickmann, K. Schmidt, B. Schuhbaur, C. Henderson, R. Blomhoff, C.R. Wolf, C. Tickle, P. Dollé, Rescue of cytochrome P450 oxidoreductase (Por) mouse mutants reveals functions in vasculogenesis, brain and limb patterning linked to retinoic acid homeostasis, Dev. Biol. 303 (2007) 66–81.
[12] N. Huang, A.V. Pandey, V. Agrawal, W. Reardon, P.D. Lapunzina, D. Mowat, E.W. Jabs, G. Van Vliet, J. Sack, C.E. Fluck, W.L. Miller, Diversity and function of mutations in P450 oxidoreductase in patients with Antley–Bixler syndrome and disordered steroidogenesis, Am. J. Hum. Genet. 76 (2005) 729–749.
[13] K. Homma, T. Hasegawa, T. Nagai, M. Adachi, R. Horikawa, I. Fujiwara, T. Tajima, R. Takeda, M. Fukami, T. Ogata, Urine steroid hormone profile analysis in cytochrome P450 oxidoreductase deficiency: implication for the backdoor pathway to dihydrotestosterone, J. Clin. Endocrinol. Metab. 91 (2006) 2643–2649.
[14] K. Takitani, H. Tamai, T. Morinobu, N. Kawamura, M. Miyake, T. Fujimoto, M. Mino, Pharmacokinetics of all-trans retinoic acid in pediatric patients with leukemia, Jpn. J. Cancer Res. 56 (1995) 400–405.
[15] G.W. Tang, R.M. Russell, 13-cis-Retinoic acid is an endogenous compound in human serum, J. Lipid Res. 30 (1990) 175–182.
[16] F.R. Goodman, P.J. Scambler, Human HOX gene mutations, Clin. Genet. 59 (2001) 1–11.
[17] K. Kosaki, R. Kosaki, T. Suzuki, H. Yoshihashi, T. Takahashi, K. Sasaki, M. Tomita, W. McGinnis, N. Matsuo, Complete mutation analysis panel of the 39 human HOX genes, Teratology 65 (2002) 50–62.

[18] R.E. Stevenson, Rectum and anus, in: R.E. Stevenson, J.G. Hall, R.M. Goodman (Eds.), Human Malformations and Related Anomalies, Oxford University Press, New York, 1993, pp. 493–499.
[19] J.S. Elder, Vesicoureteral reflux, in: R.M. Kliegman, R.E. Behrman, H.B. Jenson, B.F. Stanton (Eds.), Nelson Textbook of Pediatrics, Saunders, Elsevier, Inc., Philadelphia, 2007, pp. 2228–2234.
[20] A.L. Shen, K.A. O'Leary, C.B. Kasper, Association of multiple developmental defects and embryonic lethality with loss of microsomal NADPH–cytochrome P450 oxidoreductase, J. Biol. Chem. 277 (2002) 6536–6541.
[21] E. Batourina, S. Tsai, S. Lambert, P. Sprenkle, R. Viana, S. Dutta, T. Hensle, F. Wang, K. Niederreither, A.P. McMahon, T.J. Carroll, C.L. Mendelsohn, Apoptosis induced by vitamin A signaling is crucial for connecting the ureters to the bladder, Nat. Genet. 37 (2005) 1082–1089.
[22] R. Padmanabhan, Retinoic acid-induced caudal regression syndrome in the mouse fetus, Reprod. Toxicol. 12 (1998) 139–151.
[23] J. Gu, Y. Weng, Q.Y. Zhang, H. Cui, M. Behr, L. Wu, W. Yang, L. Zhang, X. Ding, Liver-specific deletion of the NADPH–cytochrome P450 reductase gene: impact on plasma cholesterol homeostasis and the function and regulation of microsomal cytochrome P450 and heme oxygenase, J. Biol. Chem. 278 (2003) 5895–5901.
[24] M. Uehara, K. Yashiro, K. Takaoka, M. Yamamoto, H. Hamada, Removal of maternal retinoic acid by embryonic CYP26 is required for correct Nodal expression during early embryonic patterning, Genes Dev. 23 (2009) 1689–1698.
[25] D.M. Otto, C.J. Henderson, D. Carrie, M. Davey, T.E. Gundersen, R. Blomhoff, R.H. Adams, C. Tickle, C.R. Wolf, Identification of novel roles of the cytochrome p450 system in early embryogenesis: effects on vasculogenesis and retinoic Acid homeostasis, Mol. Cell. Biol. 23 (2003) 6103–6116.
[26] M.E. Martínez Tallo, E. Galán Gómez, J.L. Cordero Carrasco, E.H. Hidalgo Barquero, F.M. Campo Sampedro, J.J. Cardesa García, Penile agenesis and syndrome of multiple abnormalities associated with the ingestion of retinoic acid by the mother, An. Esp. Pediatr. 31 (1989) 399–400 (in Spanish).
[27] G. Yamada, K. Suzuki, R. Haraguchi, S. Miyagawa, Y. Satoh, M. Kamimura, N. Nakagata, H. Kataoka, A. Kuroiwa, Y. Chen, Molecular genetic cascades for external genitalia formation: an emerging organogenesis program, Dev. Dyn. 235 (2006) 1738–1752.
[28] M.K. Cooper, C.A. Wassif, P.A. Krakowiak, J. Taipale, R. Gong, R.I. Kelley, F.D. Porter, P.A. Beachy, A defective response to Hedgehog signaling in disorders of cholesterol biosynthesis, Nat. Genet. 33 (2003) 508–513.
[29] G.E. Herman, Disorders of cholesterol biosynthesis: prototypic metabolic malformation syndromes, Hum. Mol. Genet. 12 (S1) (2003) R75–R88.